Development of a hybrid BCG:Cathepsin B vaccination strategy against *Schistosoma mansoni* infection

Esma Mouhoub

Master of Science

Microbiology & Immunology

McGill University

Montréal, Quebec

March 2023

A thesis submitted to McGill University in partial fulfillment of the requirements of the degree of Master of Science

Table of Contents

Abstract

Schistosomiasis is a human helminth infection of significant importance due to its extensive global prevalence, and severe impact on quality of life. Well above 250 million individuals are currently infected with schistosomiasis in over 78 countries, and more than 200,000 die annually due to infection related complications. Although these numbers are increasing, and greatly underestimate the disease's true prevalence, a vaccine has yet to be approved. The development of a preventative vaccine against schistosomiasis would drastically reduce disease burden and transmission. The goal of this research is to create a preventative vaccine for schistosomiasis using *Schistosoma mansoni* Cathepsin B (*Sm*CB) as a vaccine target, and *Mycobacterium bovis* Bacillus Calmette-Guérin (BCG) as an adjuvant. Two aims were conducted to fulfill this overall goal. Firstly, a recombinant BCG-*Sm*CB construct was created and S*m*CB protein expression was examined. Secondly, wild type BCG-Danish was co-administered with purified *Sm*CB protein in C57BL/6 mice. Continuing with the latter experiment, mice injected with the BCG + *Sm*CB vaccine formulation demonstrated humoral immune responses through a statistically significant increase in protective *Sm*CB-specific total IgG and IgG2c antibodies, and a slight increase in *Sm*CB-specific IgG1 antibodies. The latter indicates that the vaccine provides a mixed Th1/Th2 response with Th1 dominance. Cellular mediated immune responses were also observed in the vaccine through detectable increases in both interferon-γ (IFN-γ) and interleukin-4 (IL-4). Upon *S. mansoni* challenge, the BCG + *Sm*CB vaccine formulation led to a protective efficacy of 44.9% against Schistosoma worms, as well as a significant decrease in intestinal eggs, and a slight decrease in hepatic eggs. In closing, although further experimentation is required, this novel *Sm*CB-BCG formulation is a promising candidate for vaccination against Schistosomiasis.

Résumé

La schistosomiase est une helminthiase d'importance significative en raison de sa prévalence mondiale étendue et son impact sérieux sur la qualité de vie. Plus de 250 millions de personnes sont infectées par la schistosomiase dans 78 pays, et 200 000 meurent chaque année à cause des complications liées à l'infection. Même si ces chiffres augmentent rapidement, et sous-estiment largement la vraie prévalence de la maladie, un vaccin n'est pas encore approuvé. Le développement d'un vaccin préventif contre la schistosomiase réduirait considérablement le fardeau de morbidité et de transmission. L'objectif de cette recherche est de créer un vaccin préventif contre la schistosomiase en utilisant *Schistosoma mansoni* Cathepsin B (*Sm*CB) comme cible vaccinale et Mycobacterium bovis Bacillus Calmette-Guérin (BCG) comme adjuvant. Pour atteindre cet objectif, les études suivantes ont été menées. Tout d'abord, une construction recombinante BCG-*Sm*CB a été créée et l'expression de la protéine *Sm*CB a été tentée. Deuxièmement, le BCG-Danish a été co-administré avec la protéine *Sm*CB chez des souris C57BL/6. Poursuivant cette dernière étude, les souris injectées avec la formulation de vaccin BCG + *Sm*CB ont démontré des réponses immunitaires humorales par une augmentation statistiquement significative des anticorps IgG et IgG2c spécifiques à *Sm*CB, et une augmentation des anticorps IgG1 spécifiques à *Sm*CB. Ce dernier indique que le vaccin fournit une réponse Th1/Th2 avec une dominance Th1. L'immunité cellulaire a été observée dans le vaccin par des augmentations détectables d'interféron-γ (IFN-γ) et d'interleukine-4 (IL-4). Lors d'une infection avec *S. mansoni,* la formulation du vaccin BCG + *Sm*CB a donné une protection de 44,9 % contre les parasites *Schistosoma*, ainsi qu'une diminution significative des œufs intestinaux et une diminution des œufs hépatiques. En conclusion, même si d'autres expérimentations soient nécessaires, cette nouvelle formulation de *Sm*CB-BCG peut être un vaccin candidat efficace contre la schistosomiase.

Acknowledgements

I would like to firstly thank Dr. Reed and Dr. Ndao for choosing me for this novel project, and giving me the resources, guidance, opportunity, and courage to pursue research at a master's level. I would also like to express my very great appreciation to Dr. Domenech for her kindness, guidance, lab mentorship, and willingness to give her time so generously. Moreover, I would like to thank members of the Ndao lab, specifically Dilhan Perera, Sunny Liu, Mohamed Daoudi and Cal Koger-Pease, along with Annie Beauchamps, for continuous help with the mice experiments and immune assays. I must also thank my advisory committee, including Dr. Lopes and Dr. Veyrier, for offering valuable feedback, and teaching me to be a better critical thinker, scientific writer, and presenter. I would also like to thank all my close friends who supported me throughout my master's journey by offering comfort, compassion, invaluable advice, and memories that I will forever cherish. Finally, I would like to thank my family, Malek, Samira, Randa, Minou and Cher for their unconditional love, for always supporting me, believing in me, and motivating me to be a better person inside and outside of research.

Contribution of authors

Esma Mouhoub performed the literature searches, planned and conducted the experiments, and wrote the thesis. Dr. Pilar Domenech, Dr. Momar Ndao, Dr. Michael B. Reed and Dilhan Perera all contributed to the experimental planning. Drs Reed & Ndao proof-read the draft thesis and approved the final submitted version. I certify that, except where stated, the research described herein represents solely my own efforts.

List of abbreviations

ACK	ammonium chloride potassium lysis buffer
ANOVA	analysis of variance
APC	antigen presenting cell
BCG	*Mycobacterium bovis* bacillus Calmette-Guérin
BSA	bovine serum albumin
CD	cercarial dermatitis
CDC	centers of Disease Control and prevention
CFU	colony-forming unit
ELISA	enzyme-linked immunosorbent assay
HBSS	hank's balanced salt solution
HIV	human immunodeficiency virus
HRP	horseradish peroxidase
IDT	integrated DNA technologies platform
IFN-γ	interferon-γ
IgE	immunoglobulin E
IgG	immunoglobulin G
IL	interleukin
IM	intramuscular
IP	intraperitoneal
KS	Katayama syndrome
M. tb	*Mycobacterium tuberculosis*

NTD	neglected tropical disease
P. falciparum	*Plasmodium falciparum*
PBS	phosphate-buffered saline
RT-PCR	real-time PCR
rBCG	recombinant BCG
rcf	relative centrifugal force
SEA	soluble egg antigen
SEM	standard error of mean
*Sm*CB	*Schistosoma mansoni* Cathepsin B
T. gondii	*Toxoplasma gondii*
TB	tuberculosis
TBS	tris-buffered saline
TGF-β	transforming growth factor-β
Th	CD4+ T helper cells (Th1, Th2, Th17)
TNF-α	tumor-necrosis factor-α
Treg	CD4+ T regulatory cells
WASH	water, sanitation, and hygiene
WHO	World Health Organization

Chapter 1: A literature review of schistosomiasis and *Mycobacterium bovis* bacillus Calmette-Guérin

1.1 Schistosomiasis epidemiology

Schistosomiasis is a severe neglected tropical disease (NTD) caused by the *Schistosoma* parasitic worm. *Schistosoma* are trematode worms, that may cause fresh waterborne disease [1]. However, in contrast to other waterborne diseases, schistosomiasis infect hosts through skin contact with fresh water containing the parasite instead of direct ingestion [2]. The ability of *Schistosoma* to infect humans through skin contact leads to drawbacks in sanitation methods, such as water purifying strategies, since these methods may only protect from waterborne diseases that infect individuals through ingestion [2]. The disease has a substantial global burden. In fact, the World Health Organization (WHO) reported that at least 251.4 million people required preventative treatment in 2021, however only 75.8 million have been reported to be treated [3]. Furthermore, the WHO estimate that approximately 800 million people are at risk of infection worldwide, while over 200,000 deaths per year are attributed to disease pathology [3]. By 2021, disruptions due to the COVID-19 pandemic directly affected NTD through a large decrease in interventions and treatments for schistosomiasis [3, 4]. Specifically, the disruption of mass drug administration during COVID-19 has resulted in an increase of *S. mansoni* and *S. haematobium* species, such as the northeast Nigeria outbreak of 2020 [4-6]. Therefore, according to the WHO amongst other sources, schistosomiasis is currently the most important and devastating human helminth infection [3, 7].

Six *Schistosoma* species are proven to infect humans globally, *S. mansoni, S. haematobium, S. japonicum, S. intercalatum, S. guineensis,* and *S. mekongi* [8]. However, the geographic distribution of these species varies greatly. *S. mekongi* is localized in *Cambodia,* while *S. intercalatum* and *S. guineensis* are found in Central and West Africa [8, 9]. *S. japonicum* is endemic to parts of China, Indonesia and Southeast Asia, *S. haematobium* is found in both the Middle East and Africa, while *S. mansoni*, one of the most prevalent species of *Schistosoma*, is found in Africa, South America, Middle East, West Indies and the Caribbean [8, 10-12]. *S. haematobium, S. japonicum* and *S. mansoni* are the most common species of Schistosoma to infect humans, however *S. mansoni* is by far the most widespread [13]. In some countries with *S. mansoni* prevalence, notably sub-Saharan Africa, many children walk to school barefoot through fresh water, making them most at risk for infection [14]. Furthermore, it is estimated that 85% of all schistosomiasis cases are in Africa, with prevalence rates of over 50% in certain populations, and most travel-associated cases of schistosomiasis are from sub-Saharan Africa [15, 16]. This justifies the importance of screening and properly informing travelers of the risks associated with travel in schistosomiasis prone regions [17]. However, it is important to note that since 2018, many researchers have proved that the epidemiological statistics greatly underestimate the true magnitude of infection [18]. The inaccuracy of these statistics is predominantly due to the insensitivity and unreliability of stool analysis (the current gold standard) in detecting the presence of schistosomiasis [18-20]. Widescale insensitive detection methods lead to not only underestimation in disease prevalence, but improper measurements of efficacy of current treatments as well [18].

1.2 *Schistosoma* life cycle

The *Schistosoma* life cycle has been described by the Centers of Disease Control (CDC) and Prevention in 2019 (Figure 1) [21]. Firstly, the parasite eggs are excreted into freshwater through either the feces or urine (depending on the species of *Schistosoma*) of an infected host [21]. Under appropriate freshwater conditions the eggs (60 μm in width and 140 μm in length) hatch and release miracidia (55 μm in width and 140 μm in length) [22]. The miracidia are the free-swimming larval form of *Schistosoma*, which swim in the freshwater and penetrate the intermediate host [1]. All *Schistosoma* must infect snails as an intermediate host. However, the specific species of snails used as an intermediate differs between species of *Schistosoma*. For example, *S. haematobium* miracidia infect the *Bulinus* species, *S. japonicum* infects the *Oncomelania* species, and *S. mansoni* infect *Biomphalaria* [23]. Once *Schistosoma* infect the snail, two mother-to-daughter generations of sporocysts take place, leading to the generation of cercariae [24]. Under specific ambient temperature and light levels, the infected snails will shed cercariae of varying lengths (300 μm – 500 μm) [1].

The cercariae are the larval forms of *Schistosoma* which infect humans through skin penetration. The specific mechanisms of action that allow for penetration through human skin have been analyzed throughout the years. Lipids on the skin surface, are one of the initial triggers for invasion [25]. Furthermore, studies in *S. japonicum* have demonstrated that cysteine proteases, located in the acetabular glands of the cercariae, also induce penetration through chemical-thermal stimuli [26]. These proteolytic enzymes have been shown to degrade protein components of the immune system and epidermis, including; dermal elastin, collagen, keratin, fibronectin, immunoglobulin subclasses (A, G and M) and complement C3, thus facilitating entry and immunomodulation in the epidermis [26-28]. Upon entry in the human host, the cercariae release

glycocalyx, which allows immune evasion, shed its forked tail, and replace their tegument membranes [21, 29]. The latter allows the transformation from cercariae to schistosomula, which is the juvenile migrating larval form of *Schistosoma* [30].

The use of migration kinetics demonstrated that schistosomula stay for a mean duration of 53 hours in the epidermis, and 18 hours in the dermis [31]. However, the range of stay varies by *Schistosoma* species, since *S. mansoni* schistosomula have been shown to last up to six days in the skin [32]. Next, the schistosomula migrate to the lungs through blood flow in the venous circulation system (specifically venules in the skin) while in a semi-quiescent metabolic state [33]. Approximately two to seven days post-infection, the schistosomula arrive in the lungs [33]. Incidentally, some schistosomula acquire physical adaptations to facilitate passage through the narrow capillaries, such as the loss of the mid-body spine [34]. Travel through the host circulation systems can lead to some schistosomula getting lost. The latter either get diverted to air spaces (where they can be swallowed, digested, or coughed up), or other organs including the brain, diaphragm, and heart [35, 36]. The schistosomula leave the lungs approximately five to seven days post-infection, via the venous circulation, where some enter the portal system (through gastrointestinal capillary beds) while others re-enter the lungs (via systemic organ capillary beds) [21, 34]. Once the schistosomula reach the portal system they mature into blood-feeding juveniles in the liver, a process taking approximately three weeks [21, 37].

Once mature, the female and male adult worms mate and migrate together. The worms reside *in copula*, where the female (7.2 mm – 28 mm) is positioned inside the gynephoric canal of the male (6 mm – 13 mm) [22, 23]. The mated worms then reside in either the mesenteric veins of the

large intestine for *S. mansoni*, the superior mesenteric veins of the small intestine for *S. japonicum*, or the veins surrounding the bladder for *S. haematobium* [22]. Adult worms can live in their host for over ten years and lay hundreds to thousands of eggs per day, depending on the *Schistosoma* species. For example, *S. mansoni* females lay 100-300 eggs per day, while *S. japonicum* can lay significantly more eggs, at 500 – 3500 eggs per day [38, 39]. Furthermore, the eggs of each *Schistosoma* species exhibit specific morphological traits, thus allowing species differentiation [40]. Most eggs can then be released in feces (*S. mansoni* and *S. japonicum*) or urine (*S. haematobium*), to repeat the life cycle under appropriate fresh water conditions [21]. However, the eggs that become trapped inside the human host tissue, can lead to further disease pathogenesis [41].

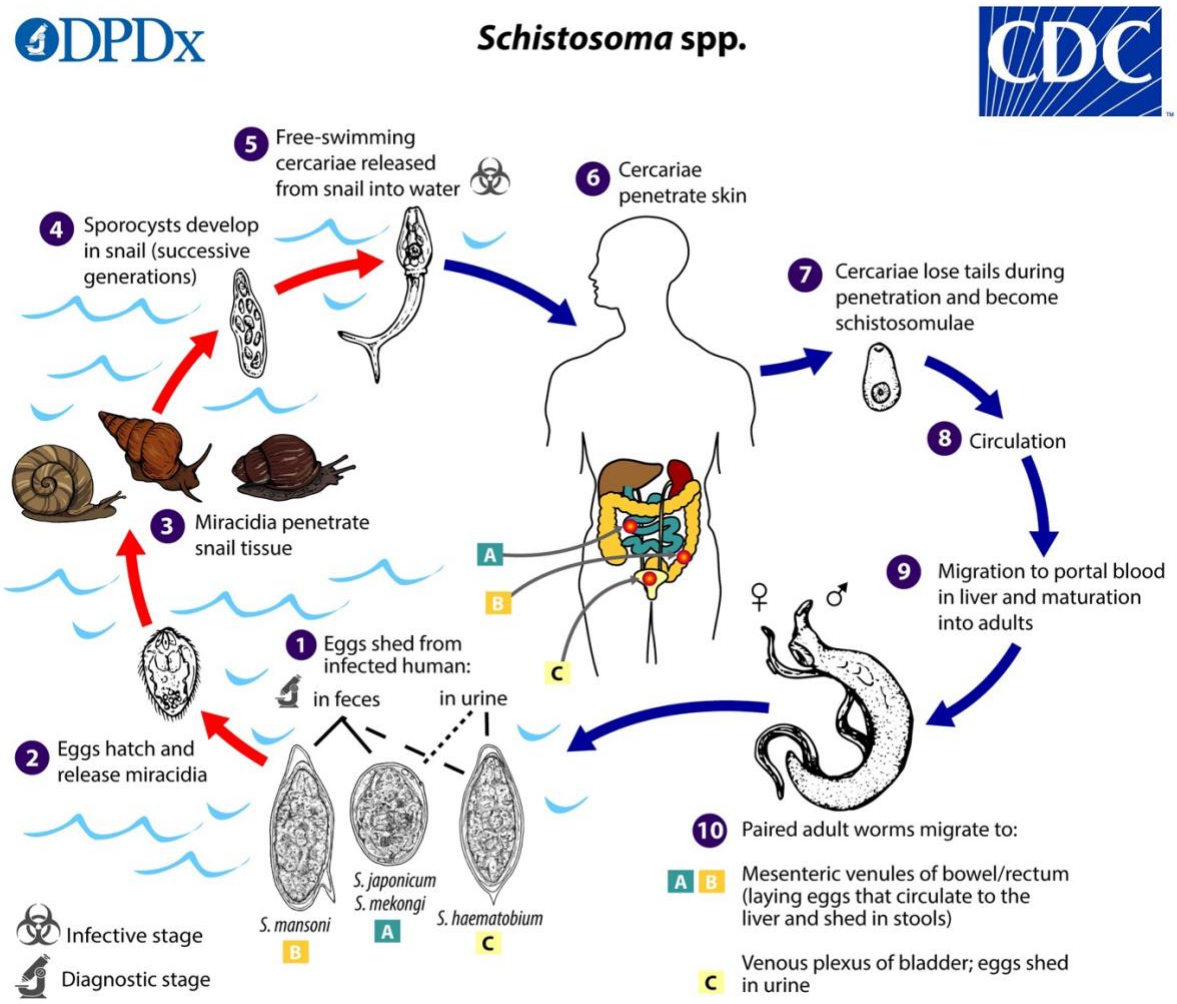

Figure 1: The Schistosoma life cycle. **1** The eggs hatch in fresh water. **2** Hatched eggs release swimming miracidia. **3** The miracidia infect snails as an intermediate host. **4** Inside the snail, sporocysts develop. **5** Sporocysts generate cercariae. **6** Cercariae swim and penetrate the human epidermis. **7** Cercariae lose forked tail upon epidermal entry and develop into schistosomulae. **8** Schistosomulae travel through the lungs, heart then develop in the liver. **9** Schistosomulae mature into male and female adult worms in the liver. **10** Male and females migrate *in copula* and reside in different locations based on the *Schistosoma* species. Females then release eggs into the freshwater, and the cycle restarts.

Figure directly obtained from Centers of Disease Control and Prevention (2019). Global Health, Division of Parasitic Diseases and Malaria. https://www.cdc.gov/dpdx/schistosomiasis/modules/Schistomes_LifeCycle_lg.jpg [42].

1.3 Schistosomiasis disease pathology

1.3.1 Acute schistosomiasis

Schistosomiasis is characterized by several short and long term effects including Katayama fever, growth stunting, ascites and renal failure, and has a substantial global burden [12]. Acute schistosomiasis is specifically indicated by Katayama syndrome (KS) and cercarial dermatitis (CD) [43]. Firstly, KS is a form of schistosomiasis mostly seen in young children and individuals with no previous exposure [44]. The symptoms of KS include non-specific symptoms such as fever, fatigue, malaise, myalgia, coughing, headaches, and swollen lymph nodes [43, 45]. However, some people may progress to a more chronic and long-term form of the syndrome, which is characterized by weight loss, rashes, and abdominal pain [45]. KS symptoms appear 14 - 84 days post exposure and are a systemic hypersensitivity reaction attributed to the migrating schistosomula and early stages of egg deposition [43, 45]. Secondly, CD, which similarly to KS is a hypersensitivity response to *Schistosoma,* is caused by the cercariae form of the parasite [46]. CD is an allergic skin disease, and its symptoms include skin blisters, rashes associated with tingling, burning or itchy sensations. The symptoms of CD appear immediately after exposure, within a few hours, and can last many days [47].

1.3.2 Chronic schistosomiasis

Incidentally, adult worms cause little to no pathology [48]. However, the hundreds to thousands of eggs released by adult females, that become trapped in host tissue, lead to chronic pathology [47]. Therefore, it is primarily the body's reaction to egg deposition that causes schistosomiasis symptoms. Chronic schistosomiasis leads to two major manifestations depending on the *Schistosoma* species. *S. mansoni* and *S. japonicum* leads to gastrointestinal diseases, while

S. haematobium leads to genitourinary diseases [47, 49]. Beginning with gastrointestinal schistosomiasis, this form of disease pathology is caused by the granulomatous responses directed towards the eggs that become trapped in the liver and intestines [50]. More specifically, the eggs trigger inflammation in these tissues, which leads to pseudeopolyposis, superficial bleeding, microulceration, and severe lesions [50]. The physical symptoms associated with liver and intestinal inflammation caused by this response, include non-specific symptoms such as abdominal pain, diarrhea, loss of appetite [51]. If left untreated, intestinal schistosomiasis can lead to the occlusion of portal veins, leading to portal hypertension [52]. The latter may be followed by more severe pathogenesis such as splenomegaly, ascites and ultimately hepatic failure due to continuous damage to the portal vein system [52]. Moving on to genitourinary schistosomiasis, eggs laid by female *S. haematobium* become embedded in the bladder and ureter walls, as well as the prostate and female genitals, thus causing calcification and fibrosis in these tissues [53]. Similarly, to intestinal schistosomiasis, the eggs trigger a hypersensitivity response, resulting in granuloma formation around the eggs, and the resulting inflammation can allow for secondary bacterial infections [54]. Symptoms may include painful urination, fever, chills and haematuria, and if left untreated can lead to renal failure [55]. Moreover, *S. haematobium* infections have been linked to both increased human immunodeficiency virus (HIV) disease progression, which is a common comorbidity in *Schistosoma* prone regions, and bladder cancer [56, 57].

1.4 Schistosomiasis immunopathology

As previously mentioned, schistosomiasis pathology results from an immune response towards the parasite eggs trapped in tissues, which act as a constant antigen stimulus [47]. The latter granulomatous response is elicited by hepatoxic soluble egg antigens (SEAs) [58]. Studies have shown that granuloma formation triggered by SEAs, and the resulting hepatic fibrosis, induces the up-regulation and expression of T- and B- cell chemoattractant which lead to the recruitment of eosinophils, neutrophils, macrophages and myofibroblasts/hepatic stellate cells [59]. Resulting granuloma formation also have protective effects. Since the eggs are hepatotoxic, granulomas release molecules that neutralizes the eggs and prevent excessive tissue damage [60]. This has been further supported by studies demonstrating that immunocompromised mice, that are unable to form granulomas, die much sooner than other mice breeds [61]. However the formation of granulomas is beneficial for the parasite as well, since it prevents premature death and therefore allows the eggs to be excreted and spread to other hosts [60].

The following analysis of Th1 and Th2 immune responses over time, follows the analysis made by Dunne *et al*'s Nature Review in 2005, (Figure 2) [62] Upon initial infection, a Th1 (CD4+ T helper cell) biased response is elicited and aimed at the adult worms for the initial six weeks [62]. The latter is characterized by the increased presence of pro-inflammatory cytokines such as tumor-necrosis factor-α (TNF-α), interleukin-1 (IL-1), IL-6, and interferon-γ (IFN-γ) [63]. However, after six weeks of infection, a predominant Th2 response emerges towards the eggs, along with suppression of the Th1 response via regulatory T cells [18, 62]. The Th2 response observed is characterized by increased levels of IL-4, IL-5, IL-10 and IL-13 [64]. Mammalian studies have demonstrated that egg deposition, which directly suppresses Th1 responses, and IL-4 are two

crucial players in skewing the host's immune responses from a Th1 towards a Th2 biased response [62]. Vaccine efficacy after helminth infection has been studied in human and monkey populations. The results of this research provide evidence that poor Th1 immunogenicity may not only be from a Th1 to Th2 shift [65]. For instance, IL-4 is responsible for not only the resulting granuloma sizes, but also the expression of lymphocytes that produce Th2 cytokines [66]. Furthermore, IL-10, which is linked to the onset of egg deposition, is responsible for down-regulating Th1 responses in chronic schistosomiasis [67]. This occurs through activation of CD4+ and CD8+ T cell apoptosis and reduces the modulation of granulomatous responses [67]. These experiments also provide evidence that increases in the activity of regulatory T cells (Tregs), IL-10 and transforming growth factor-β (TGF-β), may be the leading cause of reduced Th1 immune responses, without enhanced Th2 responses [65]. With regards to antibody titres, during cercarial challenge, IgG and IgE protective antibody titres are inversely correlated with worm burden, while IgM is positively correlated [68, 69]. IgG antibodies are known to neutralize toxins, and part of their protective effects stem from their ability to kill schistosomula [70]. Although many vaccine trials have focused on using adjuvants that solely increase Th1 responses, vaccines which elicit a mixed Th1/Th2 response, along with high protective antibody titers, result in higher levels of protection upon *Schistosoma* challenge in mice [18, 69, 71].

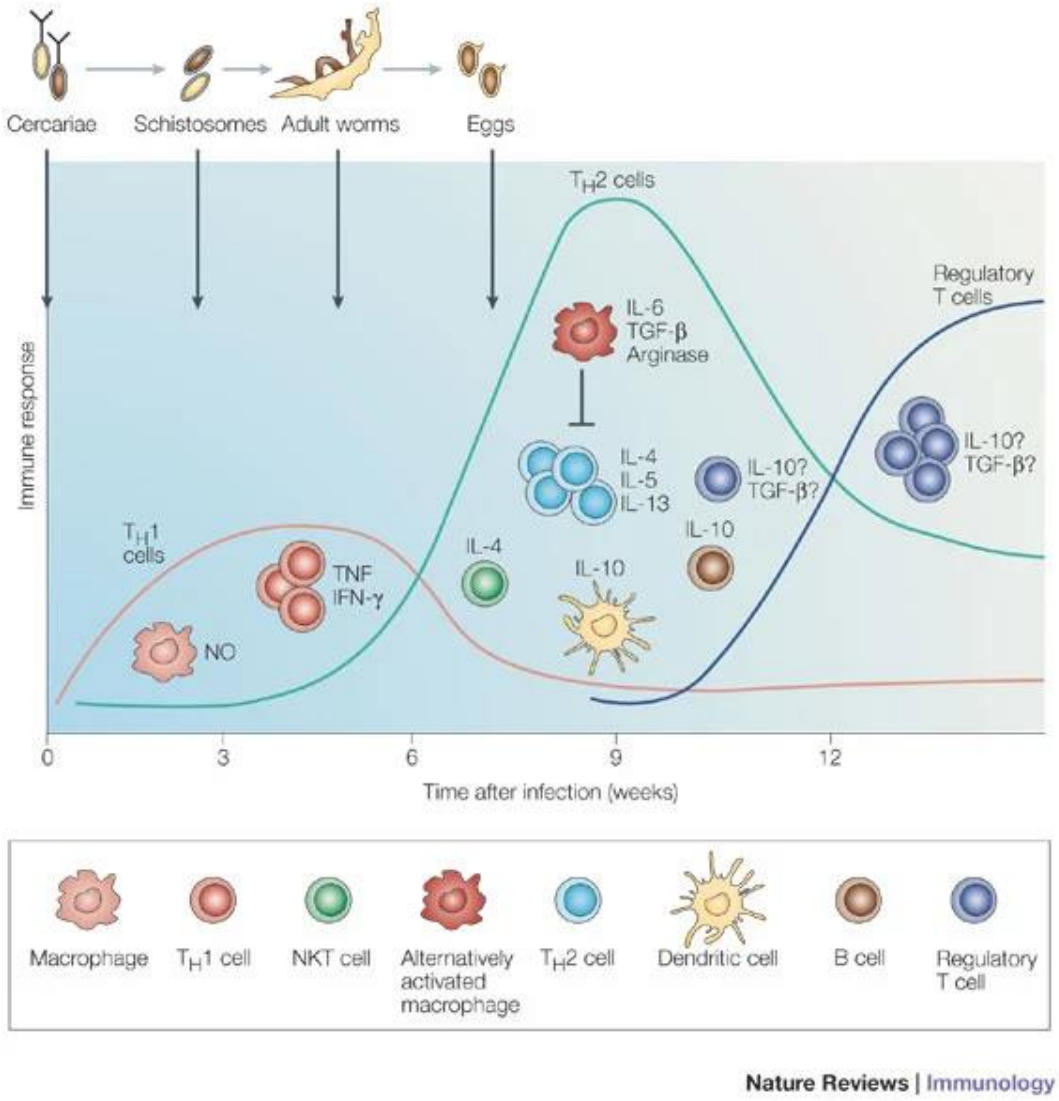

Figure 2: Cellular mediated immune responses *to S. mansoni* over time. Upon infection, a Th1 response is first directed towards the cercariae, schistosomes and adult worms. Egg deposition, and the induction of IL-10, cause a shift to a Th2 response. Finally, the expansion of regulatory T cells increases, may lead to the release of cytokines such as TGF- β.

Reproduced with permission from Springer Nature. Figure obtained from Dunne, D., Cooke, A. A worm's eye view of the immune system: consequences for evolution of human autoimmune disease. *Nat Rev Immunol* **5**, 420–426 (2005). https://doi.org/10.1038/nri1601[62].

1.5 Schistosomiasis treatment and sanitation

Praziquantel (PZQ), is the only antihelminthic FDA-approved drug of choice for schistosomiasis [72]. Benefits of PZQ include its ability to treat the three major species of *Schistosoma* (*S. mansoni*, *S. japonicum* and S. *haematobium*), along with its safety, affordability, and accessibility [73]. Unfortunately, PZQ can only target the adult *Schistosoma* worms, but not the eggs [72]. PZQ targets adult worms through two key actions of rapid contractile paralysis and tegument damage [72]. Sustained contractile paralysis occurs through Ca^{2+} influx, while tegument damage is due to erosions of tegumental integrity, and an increased exposure of worm antigen to vital host immune responses involved in worm clearance [72]. However, PZQ does present many shortcomings including undesirable side effects, the inability to protect individuals against reinfection, and increasing resistance to PZQ in *Schistosoma* prone regions [18, 67, 74, 75].

Although mass drug administration of PZQ is the current focus of most Schistosomiasis control programs, it has become more apparent that drug treatment alone is not sufficient [2, 75]. Since schistosomiasis is a water-borne disease, sanitary interventions should be taken at three key levels including reducing human contact with cercariae contaminated water, decreasing the amount of snail intermediate hosts, and blocking fresh water contamination by parasite eggs in human urine and feces [75]. To reduce human contact with contaminated waters, populations need increased access to supplies of clean water. Unfortunately, very expensive to install and maintain, and most schistosomiasis cases occur in regions with poor water, sanitation, and hygiene (WASH) conditions [76]. However, the importance of increasing good WASH conditions has been proven by countries who have eliminated schistosomiasis through economic developments leading to better WASH conditions and limiting *Schistosoma* transmission [75, 77]. Furthermore, the WHO

has recently urged the reinforcement of snail control activities for schistosomiasis reduction [3, 4]. Snail control programs aim at removing snail species capable of being a *Schistosoma* intermediate host through environmental, biological, or chemical control [3, 4]. In summary, a new more effective antihelminthic, along with ameliorated WASH, hygiene education, snail control and disease mapping, may cure the epidemic if combined with an effective preventative vaccine [74, 78, 79].

1.6 Vaccines and *Schistosoma mansoni* Cathepsin B

Unfortunately to date, no vaccine for schistosomiasis has been approved. Due to the severity and widespread presence of the disease, WHO has declared a minimum requirement of only 40% efficacy for vaccine candidates [18]. It is important to note that up until the recently WHO approved RTS,S/AS01 vaccine for malaria, there were no vaccines approved for any parasitic disease [80]. Although the efficacy of the RTS,S/AS01 vaccine differs largely based on age and dosage, its approval plays a vital role in advancing other NTD vaccines, such as schistosomiasis [80, 81]. Decades of research for potential *Schistosoma* vaccine targets has led to the analysis of multiple *Schistosoma* antigens, most of which are proteins that are either released by the parasite, surface-bound, or expressed at the parasite-host interface [82-84]. Although over 100 antigens specific to *Schistosoma* have been isolated and analyzed, only the following three antigens have begun clinical trials: *S. mansoni* fatty acid binding protein (which is used to absorb host fatty acids vital to survival), *S. mansoni* tetraspanin (abundant *Schistosom*a tegument on outer membrane) and *S. haematobium* glutathione S-transferase (enzyme used in fatty acid metabolism and immune system evasion) [82]. Therefore, more *Schistosoma* antigens should be analyzed as potential vaccine targets.

1.6.1 Cathepsin B

To provide broad protection against schistosomiasis, the cercariae and worm eggs must be targeted. Cathepsin B, a cysteine protease responsible for digestion of vital host nutrients, is abundant in the parasite's gut [69]. Due to its vital function, Cathepsin B is present in cercariae, schistosomula, worms and eggs and is vital for parasite survival, therefore making it an ideal target [74]. Cathepsin B derived from *S. mansoni* (*Sm*CB), is originally synthesized as an inactive zymogen, and becomes converted to a mature and active enzyme through a series of proteolytic processes [85, 86]. The mature form of *Sm*CB has a unique occluding loop at one end of its active cleft, which contains a catalytic dyad responsible for modulating its exopeptidase and endopeptidase activity [85, 86]. Generally speaking, proteins have been shown to make excellent antigens for vaccines due to their strong immunogenicity and the ability of their generated antibodies to recognize multiple conformational epitopes of the target protein [87]. Therefore, using the *Sm*CB protein as a schistosomiasis vaccine target may be promising.

1.6.2 SmCB vaccines

Early research conducted using *Sm*CB as a vaccine target conducted by Riccardi *et al.* demonstrated that purified *Sm*CB could induce high Th1 immune responses (characterized by elevated levels of IgG2c, IFN-γ and TNF-α) with the addition of CpG dinucleotides as an adjuvant, and a mixed Th1-Th2 response (characterized by increased IgG1, IFN-γ, TNF-α, IL-4, and IL-5) with the Montanide ISA 720 VG adjuvant (squalene-based adjuvant) [69, 88]. Both adjuvants produced significant reduction in the number of worms and intestinal eggs, with rates of up to 66%, well above the 40% threshold set by WHO [74]. More recently, higher rates of protection have been observed in novel therapeutic and prophylactic vaccine approaches using *Sm*CB. Therapeutic activity of *Sm*CB has been proven in a *Salmonella*-vectored vaccine model (attenuated

Salmonella enterica Typhimurium strain YS1646) where chronically infected mice had reduction of worms and egg with levels up to 70.3% in 2021 and 80.4% in 2023 [42, 89]. The latter vaccine model expresses *Sm*CB through promoter-type 3 secretory signal pairs to trigger a mucosal and systemic response, and mixed Th1/Th2 humoral and cellular immune responses were observed [42, 89]. Moreover, the use of AddaVax™ (AddaVax) as an adjuvant co-administered with *Sm*CB led to reduction in adult worms and eggs with levels up to 86.8%, through mixed Th1/Th2 humoral and cellular immunity [42, 90]. AddaVax is a squalene-based oil-in-water nano-emulsion similar in composition to MF59 [91, 92]. These emulsions elicit mixed Th1/Th2 immune responses by increasing antigen presenting cell (APC) activation and recruitment, as well as elevating the stimulation of granulocytes and macrophages to release chemokines and cytokines [91, 92]. The success from these different and unique vaccine candidates inspired the following research efforts using *Mycobacterium bovis* bacillus Calmette-Guérin (BCG) as an adjuvant, and recombinant BCG (rBCG) technology, combined with *Sm*CB as a potential vaccine candidate for schistosomiasis.

1.7 BCG

BCG is an attenuated form of *Mycobacterium bovis* (*M. bovis*) which is widely approved for use globally to prevent childhood tuberculosis (TB), meningitis and miliary disease [93]. The current study was designed to verify the immunogenicity and protective potential of BCG as an adjuvant when co-administered with purified *Sm*CB. BCG was chosen as an adjuvant due to its non-specific heterologous immunomodulatory effects, dominant Th1 response, heat stability, easy mass production, low cost, and safe neonatal use [93, 94]. The non-specific effects of BCG occur for both innate and adaptive immune mechanisms and may be attributed to trained immunity [95].

The latter occurs through epigenetic reprogramming of innate immune cells, after BCG exposure, and leads to specific cytokine and cell metabolism regulation [96, 97]. The BCG-Danish strain was selected due to its widespread use, especially in regions of the globe with higher schistosomiasis risk, along with its reported ability to mount significantly higher frequencies of CD4+ T cell responses and polyfunctional cytokine responses to vaccine antigens in comparison to other BCG strains [98]. Moreover, the WHO established BCG-Danish as one of three reference strains of BCG to standardize vaccine production [99]. BCG's ability to induce a robust Th1 response and non-specific immunomodulatory effects make it a successful "live-adjuvant" for combining with a variety of heterologous antigens. In the past, the direct co-administration of BCG mixed with an antigen of interest has been examined for protection against various diseases. In the case of *S. mansoni*, when paramyosin (an antigen derived from *S. mansoni)* was co-administered intradermally with BCG in mice, protection occurred through the induction of a dominant Th1 response [100]. Partial protection in worm reduction of 26–33% against *S. mansoni* challenge occurred when BCG was co-administered with only 4–40μg of the paramyosin antigen, while 2mg of the antigen alone was required to obtain the same level of protection [100]. Furthermore, in a related study in sheep, co-administration of BCG and *S. japonicum* paramyosin led to enhanced immunogenicity and up to 48% worm reduction compared to BCG alone [101]. The use of BCG as an adjuvant for *Leishmania* vaccine development has also been proven to be promising. Although previous efforts focused on combining BCG with various autoclaved *Leishmania*, more recent success was demonstrated through the co-administration of BCG and three different *Leishmania* recombinant protein peptides, which led to 75% parasite inhibition after *Leishmania* challenge and boosted cellular immune responses in golden hamsters [102-105].

1.8 Recombinant BCG technology

The following section has been adapted from my Mouhoub *et al*. (2021) mini-review publication analyzing applications of recombinant BCG technology to target infectious diseases other than TB [106]. The use of BCG as a vaccine platform *via* genetic engineering was originally described in 1991 in a landmark paper by Stover et al., demonstrating that foreign genes of interest could be introduced into BCG through the use of *E.coli-mycobacterium* shuttle vectors [107]. The latter leads to the expression of the encoded proteins either extracellularly, intracellularly, or bound to the BCG cell surface [107, 108]. To ensure a stable level of foreign antigen expression in BCG, the mycobacterial *hsp60* promoter is commonly included in plasmid expression vectors capable of integrating at the non-essential mycobacteriophage L5 attachment site [107, 108]. Additionally, optimizing the foreign gene sequences based on mycobacteria's codon-usage preferences may also increase the level of heterologous gene expression [109]. Many rBCG vaccines have already been designed for a wide range of different viral, parasitic, and bacterial antigens (including toxins) [106].

Focusing on parasitic diseases, malaria, a life-threatening disease caused by the apicomplexan parasite *Plasmodium falciparum (P. falciparum)*, has been targeted by rBCG vaccines. BALB/c mice immunized with rBCG expressing the *P. falciparum* circumsporozoite (CSp) protein demonstrated an upregulation of MHCII activation, along with CSp-specific IFN-γ producing memory cells and antibodies [110]. Mice specifically inoculated with a homologous BCG-CSp prime-boost regimen had the most robust Th1 response, characterized by higher levels of IgG2a antibodies compared to the homologous CSp/CSp recombinant protein group [110]. Although rBCG induces a predominantly Th1-type-response, Th2 responses may still be observed with rBCG parasitic vaccines. In the case of *Toxoplasma gondii (T. gondii)*, an

opportunistic protozoan parasite causing severe toxoplasmosis in humans and livestock, following vaccination with BCG expressing *T. gondii* cyclophilin (a nitric oxide inducing protein vital for the *T. gondii* life cycle) both Th1 and Th2 responses were observed in BALB/c mice prior to pathogenic *T. gondii* challenge [111, 112]. Although the Th1 response was much higher in the rBCG vaccinated groups, Th2 responses were equivalent in control (PBS or BCG) and rBCG groups [112]. Therefore, rBCG vaccination may be able to induce an enhanced Th1 response without reducing or interfering with the critical Th2 responses naturally induced against parasitic infections [112]. In the case of *S. mansoni*, rBCG expressing the Sm14 antigen (a fatty-acid binding protein) has been created and proven to induce a predominantly Th1-type-response in BALB/c or Swiss mice [109]. Furthermore, both the one or two dose regimens of the rBCG vaccine conferred a 48% reduction in worm burden upon challenge, which was comparable to three doses of the purified rSm14 antigen [109]. Therefore, the use of an rBCG vaccine platform may be promising for parasitic vaccine development, including schistosomiasis.

1.9 Project Rationale and research objectives

The ongoing lack of appropriate therapeutic drugs, ameliorated WASH, hygiene education, snail control and disease mapping in most regions with high schistosomiasis prevalence, tied in with the high disease burden caused by this disease, is more than enough proof that a vaccine against schistosomiasis is presently needed. Multiple vaccine candidates targeting *Sm*CB using various adjuvants and vaccine platforms have proven to provide protection above the 40% threshold set by the WHO in mice. This success, along with the recent progression of recombinant BCG-based vaccines for various viral, bacterial, and parasitic diseases, including *Schistosoma*

mansoni, has led to the idea of combining *Sm*CB with BCG. Therefore, through this project, I aimed to develop two experimental *Sm*CB-BCG vaccines. Firstly, through the generation of a recombinant BCG-Danish strain heterologously expressing *Sm*CB (Chapter 2). Secondly, through the use of BCG as a live adjuvant co-administered with purified recombinant *Sm*CB (Chapter 3). The efficacy of the latter was analyzed by inoculating C57BL/6 mice with the vaccine and measuring the generation of humoral immunity (through *Sm*CB-specific IgG antibodies), *Sm*CB-specific T-cells (through IFN-γ and IL-4) as well as protection against *S. mansoni* infection (through worm, intestinal egg, and hepatic egg reductions). As detailed herein, the combined BCG + r*Sm*CB vaccine elicits both humoral and cellular immunity towards *Sm*CB, and protection against *S. mansoni* infection. Thus, upon further refinement, it may in the future become a successful vaccine approach to reduce or prevent the global burden of Schistosomiasis.

Chapter 2: Recombinant BCG *Schistosoma mansoni* cathepsin B vaccine development

2.1 Materials and methods

2.1.1 Plasmid design

To address the project's initial aim, *Sm*CB DNA, codon optimized for Adenovirus (GC content of 55%), was obtained from Dilhan Perera (Ndao Lab). Various mycobacterial signal sequences have been fused to various foreign genes of interest to ensure extracellular section [113, 114]. Therefore Mpt63, an immunogenic extracellular protein abundantly expressed in mycobacteria, was chosen as a secretion signal to fuse with *Sm*CB since it met multiple important criteria [115]. First of all, when the *mpt63* sequence was run through SecretomeP2.0, it had a 99.55% probability of general secretory pathway (GSP) secretion [116]. GSP transports proteins in an unfolded state, thus preventing the creation of non-functional misfolded and aggregated proteins, and does not require the addition of chaperone proteins or accessory molecules [117]. Secondly, Mpt63 is short in length, which limits aggregation, and is also abundantly expressed and secreted in BCG-Danish [115]. Two versions of the secretion signal constructs were then designed: one with the secretion signal component from *mpt63* (mpt63sign; "signal"), and the other with the entire *mpt63* sequence (mpt63wp; "whole protein"). Furthermore, two versions of the *SmCB* DNA were designed either with or without a C-terminal histidine tag (*Sm*CB-His and *Sm*CB-NO-his respectively). Following successful PCR amplification of the individual *mpt63* and *SmCB* fragments, fusion PCR (based on the presence of overlapping sequences within the oligonucleotides used to generate these fragments) was conducted to generate a single fragment containing each *mpt63* and *SmCB* product fused together. Once the four *mpt63*-*SmCB* constructs were created, they were cloned into a self-replicating pMV361 shuttle vector [107] using *E. coli*

5-alpha cells (DH5α, New England Biolabs: C2987H). For the first plasmid (pEM-2), the latter was done through a two-step process by first cloning the insert into pMV261, then transferring the insert, along with the *hsp60* constitutive promoter contained in pMV261, into pMV306. The mycobacterial *hsp60* promoter is commonly incorporated into plasmid expression vector to maintain stable expression of foreign antigens [113, 118]. Furthermore, the plasmid is an integrative vector, meaning it integrates into a non-essential (L5 phage attachment site) region of the *Mycobacterium* chromosome [119]. The plasmids also contained a hygromycin cassette flanked with *loxP* sites. The Cre-lox system allows the exchange (or in this case, removal) of genes bearing flanking lox sequences, which are recombined through the action of the Cre recombinase enzyme to be provided on a separate plasmid [120]. Vaccines containing antibiotic genes are unsuitable for human use, predominantly due to the potential risk of horizontal transfer of antibiotic resistance to nearby microbial populations [121, 122]. Therefore, the *loxP* sites incorporated into our plasmids will be used to remove the hygromycin resistance marker. The next three plasmids (pEM-3, pEM-4 & pEM-5) were created by directly replacing the insert of either pEM-2 or pEM-3 using the *EcoRV* restriction site and either *NcoI* (for pEM-4 and pEM-5) or *HindIII* (for pEM-3) (Table 1). Following transformation into *E. coli*, all plasmids were verified through restriction enzyme digestion and Sanger sequencing to ensure the insert was free of mutations. All four plasmids were subsequently electroporated into BCG-Danish (provided by Dr. Marcel Behr; ATCC ref. 35733) and plated on Difco 7H11/OADC agar containing 50µg/ml hygromycin (Wisent). 7H11 agar (Middlebrook 7H11 agar [Difco]) was supplemented with 10% oleic acid-albumin-dextrose-catalase (OADC), which was created as per ADC (8.1 g/L NaCl, 50g/L bovine serum albumin [BSA] Fraction V [Calbiochem], 20g/L glucose), plus 0.6mL/L oleic acid and 3.6 mM NaOH.

2.1.2 Protein expression and western blot

Protein expression of *Sm*CB was analyzed through SDS-PAGE and western immunoblotting from both the rBCG cell lysates and culture supernatants. For the BCG cell pellets, the cultures were harvested through centrifugation, and washed three times using phosphate-buffered saline (PBS)-Tween 0.05% (Wisent Bioproducts). The cells were then frozen, resuspended in PBS-Triton X-100 0.1%, and proteins were extracted through the addition of approximately 0.5mL of 0.1mm glass beads (BioSpec products) and placing the tubes in the Mini-BeadBeater (6.5 m/s [4000rpm] for 30 seconds, repeated six times with 30 second breaks on ice in between). Finally, the bead-beating supernatant was subject to centrifugation through a Ultrafree-MC-GV 0.22µm filter (Millipore). To analyze the secreted proteins in the cell-free culture supernatant, 2mL of Na-deoxycholate (DOC) was added to 20mL of supernatant, shaking for 10 minutes at room temperature. Next 1.5mL of trichloroacetic acid (6% TCA) was added, shaking overnight at 4°C. The next day, the mixtures were subject to centrifugation at 5000rcf for 15 minutes at 4°C. The supernatant was then removed, and 4mL of cold acetone was added, and centrifugation was repeated. Finally, the samples were spun down, left to dry, resuspended in 40 µL of Tris (pH:8, 0.02M), and sonicated. Both the culture supernatant and cell lysate soluble (samples mixed with reducing buffer [50mM Tris 0.5M pH=6.8, 2% SDS, 5% glycerol, 0.01% bromophenol blue, 2% 2-mercaptoethanol 14.3M, and water]) and insoluble (samples in glass beads mixed with reducing buffer and 8M urea) protein fractions were verified through SDS-PAGE (12% acrylamide gel) followed by Coomassie Blue staining (Coomassie Brilliant blue G-250, AMRESCO #0615).

Subsequently, western blots were performed using the H1029 mouse monoclonal anti-His antibody as a primary antibody. Briefly, 20µL of soluble and insoluble protein fractions were loaded into a gradient (4-12%) Tris-based protein gel (Thermofisher) at 200V for 1 hour. Next the

gels were transferred to a PVDF membrane through the iBlot transblotting system (Thermofisher) and blocked with 5% Tris-buffered-saline (TBS-T)-milk, rocking for 1 hour at room temperature. After discarding the blocking solution, the H1029 monoclonal mouse anti-His antibody (Sigma-Aldrich) was diluted (using various dilutions from 1:3000 to 1:6000) in TBS-T-milk and the membrane was incubated, rocking at 4°C overnight. The following day, the membrane was washed three times with TBS-T, and the secondary antibody (rabbit anti-mouse IgG-horseradish peroxidase [HRP], Sigma-Aldrich) diluted (1:20 000) in TBS-T-milk and incubated shaking for 2 hours at room temperature. Finally, the membrane was washed three more times, and Supersignal ECL reactive A and B (Thermofisher) was added, and the membrane was exposed to autoradiography film for various times up to 1hr.

2.1.3 SmCB sequence optimization and expression in Mycobacterium smegmatis.

To try to increase *Sm*CB protein expression levels, two constructs were created with *Sm*CB optimized for *Mycobacterium* through the integrated DNA technologies platform site (IDT). Further manual edits were made to adjust to the codon preferences of *M. tuberculosis (M. tb),* particularly for alanine, arginine, serine, proline, and threonine. Three optimized versions of the mature form of the *Sm*CB protein were created (pEM-6, pEM-7 & pEM-8), as well as a control plasmid containing only the mpt63 whole protein construct without *Sm*CB (pEM-9) (Table 1). The second and third construct contained the full length optimized mature *Sm*CB, fused with either the mpt63 signal (pEM-6) or mpt63 whole protein (pEM-7). The fourth construct contained the mpt63 whole protein fused with a truncated form of *Sm*CB (270bp [serine170 to serine260] from N terminal beginning of optimized protein sequence). The truncated form of *Sm*CB has the removal of most conserved active site residues and S2 subsites (where substrates naturally bind to *Sm*CB)

to render the protein inactive but still immunogenic [123]. These four constructs were inserted into a pMV361 shuttle vector containing a hygromycin cassette flanked with loxP sites, as well as the mpt63 signal (p45-2) using *HpaI* and *NcoI* sites (Table 1, Figure 3). All four plasmids also contained a N-terminal FLAG tag for detection with an anti-FLAG antibody, a longer C-terminal histidine tag (eight histidines), and an extra stop codon at the end. These four plasmids were electroporated into *Mycobacterium smegmatis (M. smegmatis*), a non-pathogenic fast-growing strain of *Mycobacterium*, for rapid protein expression verification following the previously described plasmid and protein expression steps.

2.1.4 RNA preparation from Mycobacterium smegmatis & real-time PCR

M. smegmatis clones were cultured in 30mL of 7H9 media (Middlebrook 7H9/ADC broth containing 0.2% glycerol and 0.05% Tween-80) without BSA, and grown until they reached the early exponential phase of growth (OD_{600}= 0.3). Next the cultures were subject to centrifugation at ~2000rcf for 10 minutes at room temperature, and the pellet was frozen at -80°C overnight. The following day, 1mL of Trizol reagent (Thermofisher) was added, along with glass beads (0.1mm, Biospec products) and subject to shaking using the Mini-BeadBeater (6.5 m/s [4000rpm] for 30 seconds, repeated three times with 30 second breaks on ice in between). Next chloroform:isoamyl alcohol (24:1, Sigma-Aldrich) was added and mixed vigorously. After spinning, the aqueous phase was transferred to a tube containing 540uL of isopropanol (Sigma-Aldrich) and the RNA was precipitated for 30 minutes at -20°C. Subsequently the pellet was washed with 1mL of 75% ethanol, and RNA was resuspended in 80µL of RNase free water with Ribolock RNase Inhibitor (Thermofisher). Next the RNA was purified following the Qiagen RNA purification protocol,

subject to two DNase treatments using the Turbo DNA-free kit (Ambion # AM1907), and the presence of residual genomic DNA was verified via real-time PCR (RT-PCR) prior to cDNA synthesis. cDNA synthesis was then conducted using 0.2µg of RNA per 20µL reaction together with Superscript III reverse transcriptase according to the manufacturer's directions (ThermoFisher).

The expression levels of the clones were analyzed using RT-PCR (ABI 7300 instrument) and the SYBR Green I Dye Master Mix (Bio-Rad). Briefly, the cDNA was diluted (1:250) and 5µL was used for each reaction. The thermal cycling conditions followed were 50ºC for 2 min followed by an initial denaturation step at 95ºC for 10 min, then 40 cycles at 95ºC for 15s, 60ºC for 1 min, and data was recorded at the annealing/extension step in every cycle. Triplicates were used for each cDNA sample, and triplicate standard curves were also prepared for the *sigA*, *mpt63* and *SmCB* genes. DNA extracted from a 10mL culture of *M. smegmatis* pEM8-3 was used as calibrator since it contains full-length mpt63 and the truncated optimized *Sm*CB. The pEM8-3 DNA concentration was quantified (using the TECAN Nanoquant plate reader) and subject to four 1:4 serial dilutions to create a standard curve from 2600pg to 10.16pg, and a no template control was also added in triplicates to check for any contamination or non-specific amplification. The resulting data was then quantified relative to this standard curve as described in 2.2.4.

2.2 Results

2.2.1 Plasmid design

As previously described in section 2.1.1, nine clones were created and electroporated into BCG-Danish and *M. smegmatis* (Table 1 & Figure 3). As previously mentioned, BCG-Danish was selected for this novel recombinant vaccine experiment due to its widespread use, notable immunological effects, and since the WHO established BCG-Danish as one of three reference strains of BCG [98, 99]. BCG-Danish was originally used for plasmid electroporation and protein expression. However, since it takes approximately 4 weeks to grow viable BCG, *M. smegmatis* was later chosen for rapid protein expression verification and RT-PCR to test out the plasmids before BCG-Danish electroporation. The following three sections describe the resulting protein expression, sequence optimization and RNA analysis.

Table 1: Plasmids generated for the rBCG-*Sm*CB study. Plasmids were purified from *E. coli* (DH5α) and used to transform BCG-Danish or *M. smegmatis*.

Name	Insert	Vector	E. coli strain
pEM-1	Contains mpt63sign-*Sm*CB-NO-histag insert. A 1067 bp fusion fragment containing the 87 bp signal sequence from *mpt63* (from BCG) and 972 bp from the *Sm*CB gene was cloned into the *MscI* and *HindIII* sites of pMV261. CFU 2 was confirmed by sequencing.	pMV261	DH5α
pEM-2	Mpt63sign-*Sm*CB-NO-histag insert taken from pEM-1 and ligated with pMV306-lox-hygromycin-lox. A 1473 bp fusion fragment containing the hsp60 promoter, the *mpt63* signal and the *Sm*CB gene was taken from pEM-1. Fusion was cloned into the *XbaI* and *HpaI* sites of pMV306. CFU 4 was confirmed by sequencing.	pMV306-loxhygromycinlox	DH5α
pEM-3	Contains mpt63sign-*Sm*CB-His insert. A 936 bp fragment (containing 930 bp of the *Sm*CB gene 3' end) was removed from pEM-2 and a 957 bp *Sm*CB-His fragment (containing the same *Sm*CB gene fragment fused with a 21bp histidine tag) was inserted into the *EcoRV* and *HindIII* sites of pEM-2. CFU 7 was confirmed by sequencing.	pEM-2	DH5α
pEM-4	Contains mpt63wp-*Sm*CB-NO-histag insert. A 92 bp fragment (containing 44 bp of the *mpt63* signal sequence and 48bp of the 5' end of the *Sm*CB gene) was removed from pEM-2 and a 482 bp fragment (containing 434 bp of the *mpt63* whole protein sequence, and 48bp of the 5' end of the *Sm*CB gene) was inserted into the *NcoI* and *EcoRV* sites of pEM-2. CFU 7 was confirmed by sequencing.	pEM-2	DH5α
pEM-5	Contains mpt63wp-*Sm*CB-His insert. A 92 bp fragment (containing 44 bp of the *mpt63* signal sequence and 48bp of the 5' end of the *Sm*CB gene) was removed from pEM-3 and a 482 bp fragment (containing 434 bp of the *mpt63* whole protein sequence, and 48bp of the 5' end of the *Sm*CB gene) was inserted into the *NcoI* and *EcoRV* sites of pEM-3. CFU 4 was confirmed by sequencing.	pEM-3	DH5α
pEM-6	Contains mature *Sm*CB optimized for Mtb and mpt63 signal pMV306-hsp60-loxphygloxp-mpt63sign vector (45) A 862bp fragment containing optimized mature *Sm*CB and mpt63 signal was inserted into the HpaI and NcoI sites of 45 CFU 1 and 4 were confirmed by sequencing	45	DH5α
pEM-7	Contains mature *Sm*CB optimized for Mtb and whole protein mpt63 pMV306-hsp60-loxphygloxp-mpt63sign vector (45) A 1243bp fragment containing optimized mature *Sm*CB and mpt63 whole protein was inserted into the HpaI and NcoI sites of 45 CFU 2 and 6 were confirmed by sequencing	45	DH5α
pEM-8	Contains truncated form of mature *Sm*CB optimized for Mtb fused with the mpt63 whole protein sequence pMV306-hsp60-loxphygloxp-mpt63sign vector (45) A fragment containing optimized truncated mature *Sm*CB (888bp fragment from the 5' end) was inserted into the HpaI and NcoI sites of 45 CFU 1 and 3 were confirmed by sequencing	45	DH5α
pEM-9	Contains whole protein mpt63 pMV306-hsp60-loxphygloxp-mpt63sign vector (45) A 490bp fragment containing mpt63wp was inserted into the HpaI and NcoI sites of 45 CFU 1 was confirmed by sequencing	45	DH5α

A

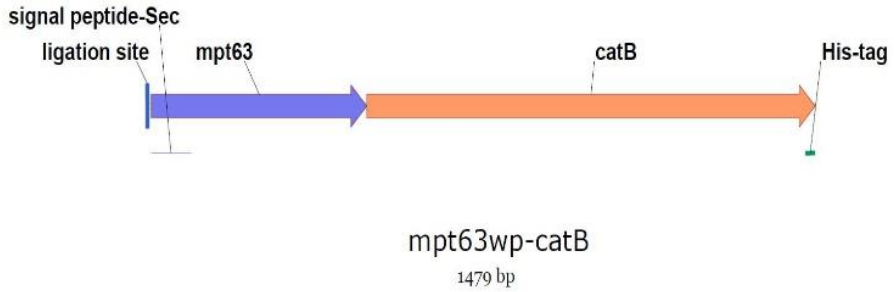

B

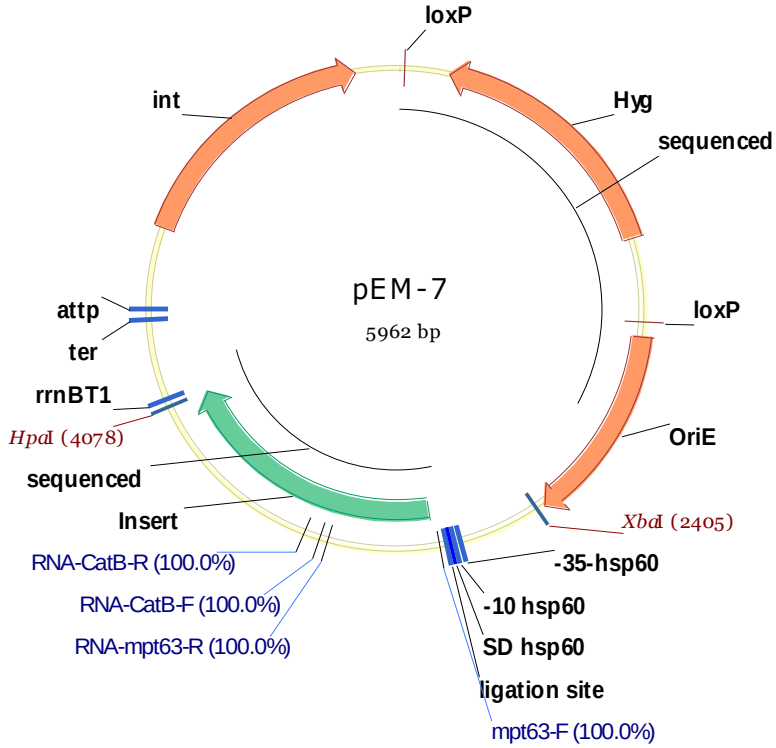

Figure 3: A schematical representation of one insert and plasmid map used for the rBCG-*Sm*CB study. All constructs and plasmids were created using Vector NTI Advance. **1A:** Insert of mpt63 whole protein fused with *Sm*CB containing a histidine tag. The signal-peptide-Sec represents the secretion signal portion of mpt63. **1B**: pEM-7 plasmid map. The pEM-7 plasmid contains full-length *Mycobacterium* optimized *Sm*CB fused with whole protein mpt63, which was verified through sanger sequencing. The plasmid contains a hygromycin cassette flanked with loxP sites that was also verified through sanger sequencing. Primers used in the RT-PCR study are labeled, as well as the *XbaI* and *HpaI* ligation sites used for cloning of the insert.

2.2.2 Protein expression and western blot

The BCG clones containing pEM-3 were chosen for the initial western blots as they contain the signal portion of mpt63, and a histidine tag that can be targeted with anti-His antibodies (Table 1). After the presence of proteins were verified via Coomassie gel, western blots were run to analyze the presence of *Sm*CB proteins using anti-histidine antibodies. The samples were run alongside a positive control containing an unrelated protein fused with a histidine tag (rabies virus protein obtained from Dr. Pilar Domenech), and a negative control containing the cell pellet of BCG clones with the pEM-2 plasmids (containing the mpt63 signal fused to *Sm*CB with no histidine tag) (Table 1). The expected size for our protein was 41kDa, and the expected size for the positive control was 53.7kDa. In the western blot a dominant single band was present at approximately 50kDa in all the samples, except for the insoluble negative control (Figure 4). While several other very faint bands could also be observed, there were none that were specific to the BCG::pEM3 clones. Therefore, western blots were repeated following the same steps for BCG-Danish electroporated with pEM-5 (which contains a histidine tag and the whole protein mpt63). Unfortunately, the same trend appeared for pEM-5 in which a 50kDa band was present in all soluble and insoluble cell fractions, except for most of the insoluble negative controls, meaning that our 41kDa protein could be the 50kDa protein band observed in the insoluble fraction, or it may be a different 50kDa protein. Additional western blots conducted under various other conditions were performed, including analyzing proteins from the cell supernatant, are further described in the discussion, and all led to the same trend being observed. Therefore, since protein detection was inconclusive for pEM-3 and pEM-5, we decided to try to optimize the *Sm*CB DNA for *M. tb* to create new clones and attempt to increase *Sm*CB protein expression.

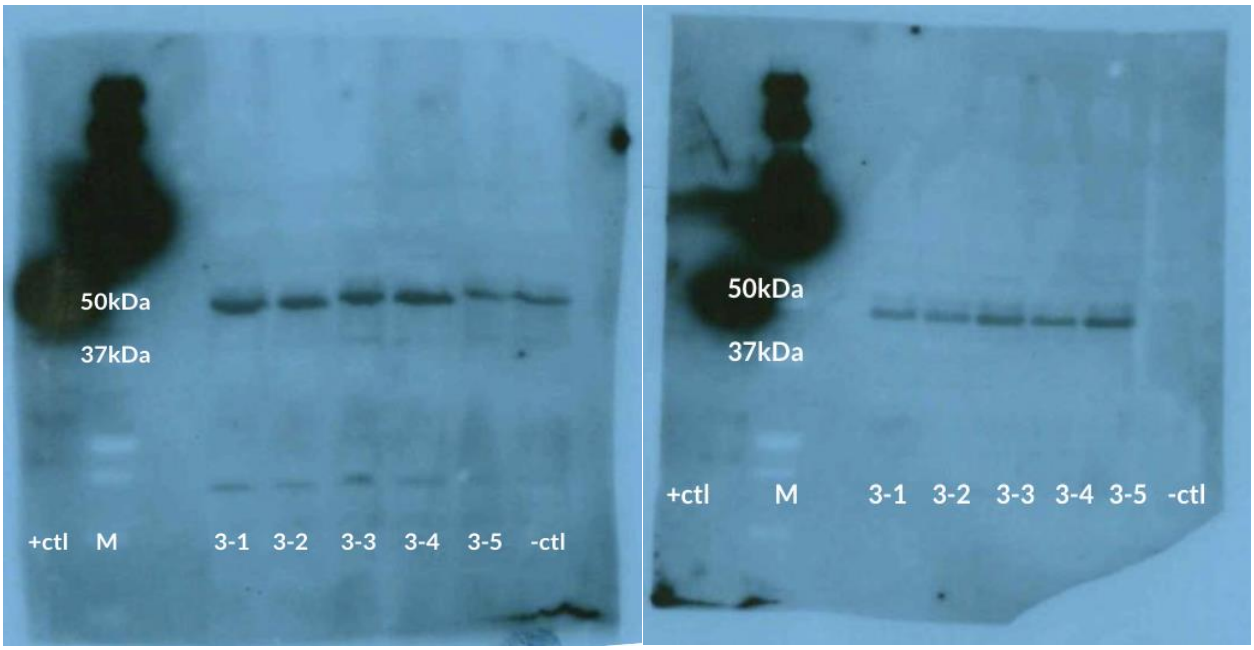

Figure 4: Western Blot for the soluble and insoluble protein fractions derived from pEM-3 cell pellets. The proteins were transferred to a PVDF membrane and a 1:6,000 dilution of the H1029 anti-His primary antibody was used, followed by a rabbit anti-Mouse IgG (HRP secondary antibody, 1:20,000 dilution), and exposed to autoradiography film for 1 hour. The pEM-3 soluble protein fractions are on the left, while the insoluble fractions are on the right. For both membranes the order of sample loading is positive control, molecular-weight ladder, 5 clones of pEM-3, negative control. The ladder marker is labeled as "M".

2.2.3 SmCB sequence optimization

The *Sm*CB DNA was codon optimized for *M. tb* as described in the Materials and Methods (Supplemental Table 2.1). The ratio of specific codon usages for the amino acids varies significantly for certain amino acids (specifically Alanine, Arginine and Threonine) between the *Sm*CB optimized for Adenovirus, and the *M. tb* genome. Therefore, the optimized *Sm*CB DNA sequence was used for RT-PCR and subsequent attempts at protein expression verification. The latter was done by electroporating *M. smegmatis* with the new optimized plasmids, specifically pEM-6, pEM-7, pEM-8 & pEM-9 (Table 1). As previously mentioned, these plasmids contain both a longer C terminal histidine tag, and a N terminal flag tag. In addition, the pEM-8 and pEM-9 constructs are expected to express proteins that are considerably smaller than 50kDa, which would avoid the possibility of co-migration (ie. our protein of interest migrating at the same rate as the unwanted 50kDa protein). Furthermore, since *M. smegmatis* grows a lot quicker than BCG-Danish, it was chosen for rapid protein expression verification. Following the previously mentioned Coomassie gel and western blot steps, unfortunately all attempts using optimized *Sm*CB led to the same inconclusive results. As further described in the discussion, as per Fig. 4, a 50kDa band was consistently observed in all samples of the western blots, including the negative controls, when using either anti-histidine antibody or anti-flag antibodies (data not presented).

2.2.4 RNA preparation from Mycobacterium smegmatis & real-time PCR

Since repetitive western blots gave inconclusive results for protein expression, verifying gene expression via RT-PCR was conducted next. The insert portion of the optimized clones were verified through sanger sequencing, which meant that these clones were successfully electroporated into *M. smegmatis*. Therefore, since the proteins were not being detected, RNA was extracted from these clones to evaluate whether the transcription or translation is being impeded.

Gene expression for *M. smegmatis Sm*CB clones pEM7-2, pEM7-6, pEM8-3, and the p45-2 empty vector was measured using relative quantification based on the std. curve method (relative to the *M. smegmatis* pEM8-3 standard curve) [124]. Expression of the *SmCB* and *mpt63* genes within the recombinant *M. smegmatis* clones was normalized to the constitutively expressed *sigA* gene [125]. Both *mpt63* and *Sm*CB portions of the construct were strongly expressed in pEM7-2, pEM7-6 and pEM-8 clones (Figure 5).

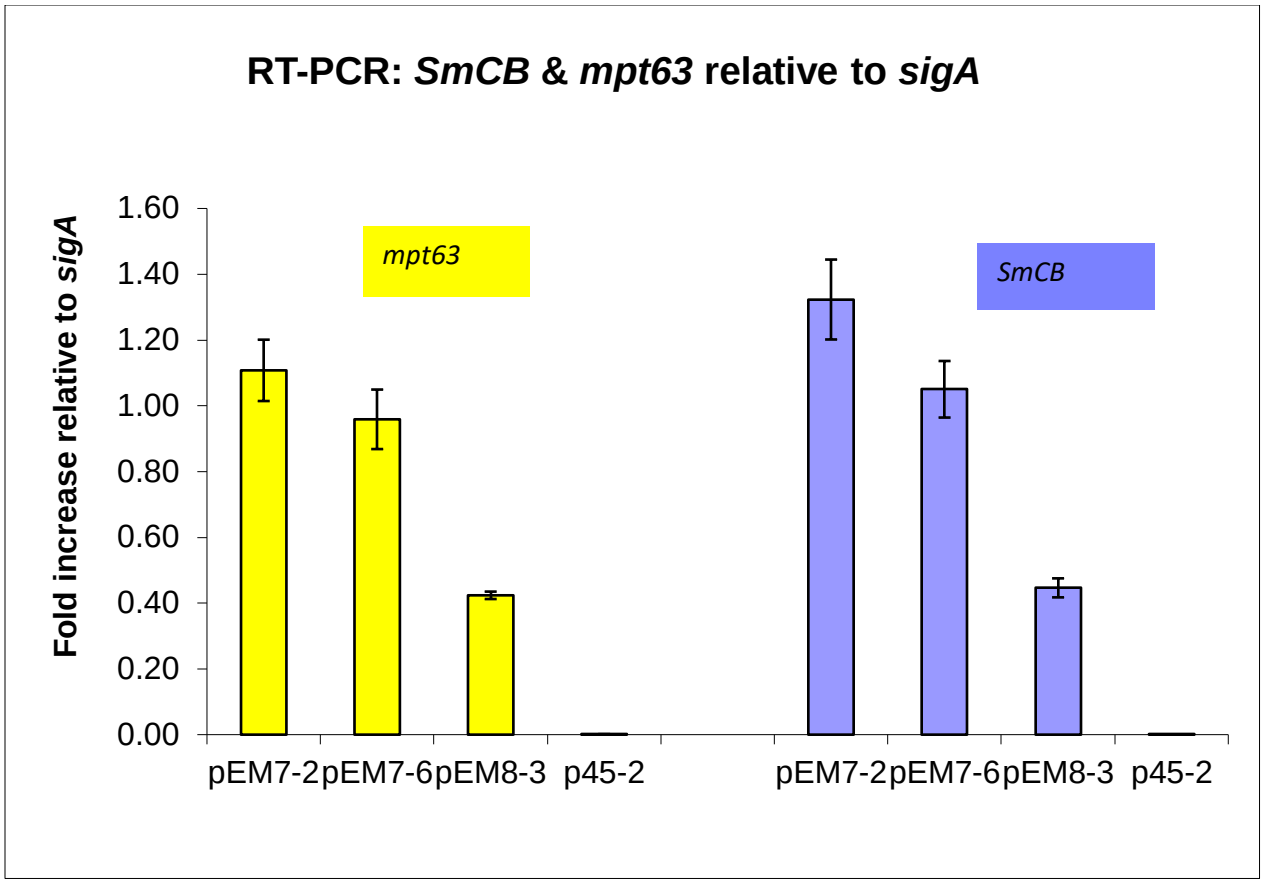

Figure 5: RT-PCR analysis of *SmCB* and *mpt63* gene expression relative to *sigA*. Expression was quantified relative to *sigA*. pEM7-2 & pEM7-6 are both two clones from the pEM-7 plasmid (containing mpt63 whole protein and optimized full-length *Sm*CB). pEM8-3 contains the mpt63 whole protein and optimized truncated *Sm*CB, while p45-2 is an empty vector. The error bars represent the standard deviation from the triplicates.

2.3 Discussion

Multiple western blots were conducted to verify protein expression of all clones (including clones with *Sm*CB DNA optimized for *Mycobacterium*) from both rBCG and *M. smegmatis* cell pellets and culture supernatants. Unfortunately, a pattern occurred for multiple western blots where a clear band at approximately 50kDa was present in both the samples and most negative controls when using anti-histidine antibodies. This was unexpected since the negative control did not contain a histidine tag. Therefore, the negative control, along with our samples, may have a *Mycobacterium* protein containing multiple histidines (such as *Mycobacterium* GroEL subunits which are around 57kDa) that is reacting with the anti-His antibody, or there is some other unexpected cross-reactivity [126, 127]. While it is theoretically possible that the full-length mpt63-*Sm*CB fusion may have the same mobility as the 50kDa band under the conditions tested, we never saw clear evidence of this. We also never saw evidence of the shorter constructs being expressed at the protein level (eg. pEM8 expressing a truncated version of *Sm*CB) with either the anti-His, nor anti-FLAG antibodies. It is also important to note that the unwanted 50kDa protein was mostly present in the negative controls from the soluble fractions, but less frequently present in negative controls from the insoluble fractions (Figure 4). Additional western blots were conducted using proteins derived from rBCG constructs without *Sm*CB or histidine tags to verify additional negative controls, and the same 50kDa band was observed in most of the soluble fractions but not always the insoluble fractions, further supporting that the protein observed may be a soluble GroEL subunit [128, 129]. Furthermore, *Sm*CB serum was used as a primary antibody to attempt to detect the *Sm*CB protein. Purified *Sm*CB was used as a positive control, and the negative control contained BCG pellets with a plasmid containing the mpt63 signal but no *Sm*CB. Unfortunately, the serum antibody was not very specific, so multiple bands at similar sizes were present in the

samples and negative control (data not shown). Another issue in rBCG-*Sm*CB protein expression may be the placement of the histidine tag, since it was placed at the C terminal of the insert, it may be cleaved post-translationally [130]. However, when running western blots using anti-FLAG primary antibody instead, for the optimized clones containing a N terminal flag tag, protein expression was still not being detected.

To further investigate at which step rBCG-*Sm*CB protein expression is hindered, PCR, sanger sequencing and RT-PCR were conducted. As mentioned previously, all clones had the insert portion of the rBCG-*Sm*CB DNA completely sequenced to verify that it was cloned correctly and that there were no mutations, including in the upstream control sequences of the plasmid (Table 1). Since cloning was proven to be successful, but we could find no consistent evidence of the protein being expressed using a range of approaches, RNA from pEM-7 (containing full length mature *Sm*CB), pEM-8 (containing truncated *Sm*CB) and p45-2 (an empty vector control) were analyzed from specific clones to verify if transcription was successful. As expected, expression of both *Sm*CB and mpt63 were observed for pEM-7 and pEM-8, but not p45-2. Moreover, two pEM-7 clones (pEM7-2 and pEM7-6) had expression levels of both *Sm*CB and mpt63 equal to or above that of the constitutively expressed *sigA* gene. Therefore, the optimized mature form of *Sm*CB may be ideal to focus on in future rBCG-*Sm*CB experiments since it is being expressed more than the truncated form. However, the optimizing of *Sm*CB DNA may not have increased protein expression as much as expected due to a recent study demonstrating that since the translational machinery of an organism, namely *M. tb*, co-evolves with the specific codon usage to conduct efficient translation, then maladapted codons have relatively no effect on translational efficiency [131].

In conclusion, it seems that rBCG-*Sm*CB cloning, and transcription was for the most part successful in *M. smegmatis* and BCG-Danish. However, the precise reasons why we could not detect protein expression remain elusive. The three most likely explanations seem to be that the protein is deleterious to the cells and is expressed at very low levels, *ie*. below the detection limit of the chemiluminescent detection system used herein. Alternatively, one or more cleavage events is occurring to the protein such that the HIS and/or FLAG tags are no longer present. Third, the protein is toxic to the cell and is rapidly being degraded. *Mycobacterium* may not be the best recombinant protein expression system for *Sm*CB, and potentially for other heterologous proteins. The latter is supported by the ability of *E.coli*, a commonly used recombinant protein expression system, to increase expression of multiple mycobacterial membrane proteins compared to *M. tb* [132, 133]. For the former, multi-copy plasmids are typically used for protein-expression work. However, in our case we are using a single-copy plasmid that is integrated into a non-essential region of the BCG or *M. smegmatis* chromosome. As our original intention was to use the rBCG approach for vaccination purposes, we chose not to investigate the use of episomal, non-integrated plasmids that have a much greater potential to be lost when not selected for. Furthermore, the expression vector used has previously been demonstrated to work in our lab for protein expression in BCG via western blot, as the same plasmid backbone including the mpt63 signal is sufficient to express a truncated form of the SARS-Co-V2 Spike protein (Dr. Pilar Domenech; unpublished data). Therefore, the protein expression complications are not due to the plasmid itself. However, as previously mentioned, since the use of other recombinant *Sm*CB bacterial vaccine models, such as using *Salmonella* as a vector, led to reduction of worms and liver eggs up to 80.4% in chronically infected mice, it would be beneficial to use other recombinant bacterial vaccine models as well [89]. Also, in order to definitively determine whether our protein of interest was being expressed

or not, it would be necessary to send purified proteins from the rBCG-*Sm*CB clones for mass-spectrometry based proteomics [134]. Regardless, it was clear from the Western blotting that even if our *Sm*CB protein was being expressed at minute levels, this was very likely not going to be sufficient to generate a strong anti-*Sm*CB immune response, let alone one that was going to be protective upon challenge with *S. mansoni*. Therefore, due to the ongoing difficulties with protein expression in the rBCG-*Sm*CB vaccine project, a parallel secondary project, was implemented to verify the immunogenicity and protective efficacy of BCG as an adjuvant when co-administered with purified *Sm*CB, as described in Chapter 3.

Chapter 3: Evaluation of BCG co-administered with *Schistosoma mansoni* cathepsin B in C57BL/6 mice

3.1 Materials and methods

3.1.1 SmCB recombinant protein expression

Pichia pastoris yeast transformed with a vector (pPinkα-HC vector) expressing *Sm*CB (containing a histidine tag) suitable for yeast expression was obtained from the Ndao lab. The *Sm*CB expression was done following the PichiaPink protocol (Thermofisher). Briefly, a yeast starter culture was created in a buffered complex glycerol medium using BMGY base (yeast extract, H_2O & peptone), 10% glycerol, K+ buffer (1M K_2HPO_4 & 1M KH_2PO_4), 13.4% yeast nitrogen base (H_2O, YNB containing $[NH_4]_2SO_4$ & amino acids), 500x biotin, and 1.0mL of frozen *Pichia pastoris*-*Sm*CB yeast. The starter culture was placed in a shaking incubator at 28°C and 250rpm until it reached log phase growth (OD_{600}=6), which took two days. Next the cells were centrifuged at 3000rcf at room temperature for 10 minutes, and the cell pellet was resuspended in the same buffered complex medium as before but with the addition of 1% methanol and the removal of glycerol. The culture was placed in a shaking incubator at 28°C and 250rpm for three days, and 1% methanol was added every 24 hours.

The cells were then centrifuged at 3000rcf at room temperature for 5 minutes, and the supernatant filtered once through a 0.2µm filter. The supernatant was then diluted 1:4 in column buffer (pH=8.0, 300mL 1M NaCl, 50mL 1M Sodium phosphate, 10mL Imidazole, water to 1L) and the pH was adjusted to pH=8.0 with NaOH, and the following purification and dialysis steps were all conducted at 4°C. To purify the protein using Ni-NTA affinity chromatography, a purification column containing 3mL slurry Ni-NTA agarose beads (Thermofisher) was set up and

equilibrated by passing through 30mL of column buffer. The supernatant was then passed through a pump into the column for 1-2 hours. Next the column was washed with 40mL of wash buffer (pH=8.0, 150mL 1M NaCl, 25mL 1M Sodium phosphate, 10mL 1M Imidazole, water to 500mL), and the eluate was collected by adding 10mL of elution buffer (pH=6.0, 12mL 1M NaCl, 2mL 1M Sodium phosphate, 14mL 1M Imidazole, water to 40mL). The eluate was then rotated for 30 minutes and left to rest for 10 minutes, and this elution and rotation step was repeated three times. Dialysis was then conducted by first rotating a 30mL Slide-A-Lyzer dialysis cassette (10K MWCO, Thermofisher) in 4L 1xPBS (10xPBS; pH=7.4, 160g NaCl, 4g KCl, 28.8g Na_2HPO_4, 4.8g KH_2PO_4 and water to 2L) bucket for 10 minutes. Next a 20mL syringe and 23G needle were used to aspirate the eluate and transfer it into the cassette, and excess air was removed. The cassette was then rotated for 3 hours in covered 4L 1xPBS, then replaced with fresh 1xPBS and rotated overnight. The following morning, the 1xPBS was replaced one more time, and the cassette rotated for another three hours. Moving back to room temperature, the eluate liquid was aspirated from the cassette, transferred into an Amicon tubes (MilliporeSigma Amicon ultra-2 centrifugal filter unit), centrifuged for 2440 rcf at room temperature for 13 minutes and 100uL aliquots were created. Finally, the BCA protein assay (Thermofisher) and a western blot using anti-His tag antibodies as described above, were conducted to quantify and verify protein expression.

3.1.2 BCG inoculum stock preparation

Wild-type BCG-Danish inoculum for vaccination was prepared for both the immunogenicity and challenge studies. Briefly, a frozen wild-type BCG-Danish stock was thawed and grown in regular 7H9/ADC media (see above) until it reached the exponential phase of growth (OD_{600}= 0.6 ~ 10^8 colony-forming unit [CFU]/mL). The culture was subject to centrifugation at 2,000rcf for 20 minutes at room temperature. Next, the pellet was washed with 10mL of wash

buffer (PBS + 0.05%Tween80), and the spin and wash step were repeated a second time with 10mL wash buffer, and a third time with 6mL of wash buffer. The resuspended culture was then passed ten times through a 22G-1" needle, then another ten times through a 27G needle. Next 6mL of culture was mixed with 4mL of sterile 50% glycerol in PBS and aliquots were frozen at -80°C.

For week 0 and week 6 for both the immunogenicity and challenge studies, frozen aliquots were diluted and mixed with PBS-Tween80-0.05% to obtain ~ 1.00 x 10^6 CFU of BCG per mouse. To verify the exact amount of BCG given per mouse, six 10-fold serial dilutions from the frozen BCG-Danish aliquots were created, and 100µL from each dilution was plated on 7H11/OADC and incubated for 4 weeks at 37°C. Afterwards, the number of colonies was counted, and the average count was determined. The plating and counting from the frozen aliquot were repeated on the morning of each inoculation.

3.1.3 Mice

All animal procedures were performed in accordance with Institutional Animal Care and Use Guidelines and were approved by the Animal Care (Animal Use Protocol 7625) and Use Committee at McGill University. The genetic background of the mice is important in analyzing Th1/Th2 balance. Research has supported that C57BL/6 mice seem to favour Th1 cytokine (high IFN-y and low interleukin IL-4) while BALB/c mice prefer Th2 cytokine (low IFN-y and high IL-4) [135]. In addition to Th1 or Th2 dominance, the main applications of these mice differ, where C57BL/6 mice are advantageous for pathological *in vivo* experiments, while BALB/c mice are excellent models for cancer therapy [136]. C57BL/6 mice may be preferable for this prime-boost strategy due to their use in previous *Sm*CB vaccine strategies, along with their Th1 dominance [74].

3.1.4 Immunogenicity study

Twenty-five 6–8-week-old female C57BL/6 mice were purchased from Charles River Laboratories (Senneville, QC). All mice were inoculated intraperitoneally (IP) at week 0 and week 6 with the same 450µL vaccine formulation for each respective group, using 25G needles (Table 2). All vaccine formulations were created by vortexing the required components until a homogenous mixture was obtained. Group 1 had four mice inoculated with 20µg of purified *Sm*CB in PBS-Tween80-0.05% (Wisent Bioproducts). Group 2 had three mice inoculated with 25µL of AddaVax (Invitrogen) in PBS-Tween80-0.05%, while group 3 contained five mice inoculated with 20µg of purified *Sm*CB & 25µL of AddaVax in PBS-Tween80-0.05%. Group 4 had five mice inoculated with ~ 1.00 x 10^6 CFU BCG-Danish in PBS-Tween80-0.05%, and group 5 had five mice inoculated with ~ 1.00 x 10^6 CFU BCG-Danish, 20µg of purified *Sm*CB in PBS-Tween80-0.05%. Lastly, group 6 acted as a saline control by inoculating three mice with PBS-Tween80-0.05%. The concentrations of purified *Sm*CB and AddaVax were based on previous IM vaccines done by the Ndao lab [137]. Unfortunately, approximately 4 weeks into the experiment, one mouse died from group 5. The cause of death was unknown, and the mouse showed no previous signs of illness. Therefore, the group 5 data is from four mice instead of the original five. Furthermore, all mice were weighed at weeks 0, 6 and 10 to ensure healthy body condition (Supplemental Figure 3.1).

3.1.5 Challenge study

Similarly, to the immunogenicity study, twenty 6–8-week-old female C57BL/6 mice were purchased from Charles River Laboratories (Senneville, QC), and all mice were inoculated IP at week 0 and 6 with 450µL of each vaccine formulation (Table 2). However, the groups were

modified such that four groups of five mice each were created. Group 1 had 20μg of purified *Sm*CB in PBS-Tween80-0.05%. Group 2 had ~ 1.00 x 10^6 CFU in PBS-Tween80-0.05%, while group 3 contained ~ 1.00 x 10^6 CFU in PBS-Tween80-0.05% mixed with 20μg of purified *Sm*CB. Finally, group 4 acted as a saline control where mice were inoculated with PBS-Tween80-0.05%. Similarly, to the immunogenicity study, all mice were weighed at weeks 0, 4, 9 and 15 to ensure healthy body condition (Supplemental Figure 3.2).

3.1.6 Schistosoma mansoni challenge

Biomphalaria glabrata snails infected with the Puerto Rican strain of *S. mansoni* were originally obtained from the Schistosomiasis Resource Center of the Biomedical Research Institute, then maintained in the Ndao lab. For the challenge study, four weeks after the second vaccine injection (week 10), all mice were challenged with 150 cercariae via tail exposure. The cercariae were first shed from the snails by placing the snails in a small beaker containing fresh spring water for 40 minutes. The cercariae water was then placed in a 50mL falcon tube, five 10μL drops were placed on a petri dish, and the cercariae were counted under the microscope. The average counted from the 5 drops was then used to calculate how much cercariae water to use per mouse to ensure approximately 150 cercariae were given (spring water was added to the cercariae water to reach a total volume of 13mL for each 15mL tube). Each mouse was placed inside a vertical retainer with their tail inside the 15mL falcon tube containing 150 cercariae in spring water for 1 hour [138]. Seven weeks after challenge, the mice were sacrificed, and adult worms were perfused from the hepatic portal system and counted manually by euthanizing the mice, severing the hepatic portal vein, and pumping perfusion fluid (0.85% sodium chloride + 0.75% sodium citrate) to collect the worms. The liver and intestines were also weighed and digested overnight at

37°C in 4% potassium hydroxide. One day later, eggs in both these tissues were counted by microscopy and the number of eggs per gram of tissue was estimated. The latter was done by mixing the tube, placing five 10μL drops on a petri dish, and counting the amount of eggs under the microscope to calculate the average number of eggs, Lastly, the reduction in egg and worm burden were calculated using the formula below:

$$\%\ eggs\ or\ worms\ reduction = \left(1 - \frac{mean\ \#\ of\ worms\ or\ eggs\ recovered\ in\ vaccinated\ mice}{mean\ \#\ of\ worms\ or\ eggs\ recovered\ in\ PBS\ control\ mice}\right) \times 100\%$$

3.1.7 Quantification of humoral response by indirect enzyme-linked immunosorbent assays (ELISA)

Throughout both the challenge and immunogenicity study, saphenous blood was collected from all mice at week 0, 6 & 10. Furthermore, for the challenge study, saphenous blood was also collected at weeks 12, 14 and 17. The sera was obtained by centrifugation at 10,000rcf for 8 minutes and humoral responses were measured through ELISA. First, 96 well U-bottom plates (Greiner Bio-One) were coated with 0.5μg/mL per well of purified *Sm*CB protein and incubated overnight at 4°C. A standard curve containing 1:2 serial dilutions from 2000ng/mL to 2ng/mL for each IgG antibody subtype (IgG, IgG1 or IgG2c, Sigma-Aldrich) was plated for every trial as well. The next day, plates were washed three times with 1xPBS (pH 7.4; 0.01M phosphate buffer, 0.14M NaCl) containing 0.05% Tween20 (Sigma-Aldrich). Plates were then incubated for 1 hour at 37°C with 100μL/well of blocking buffer (1xPBS & 5% bovine serum albumin) (Sigma-Aldrich). The mice sera were diluted in blocking buffer in duplicates (1:50 for IgG, IgG1, and 1:25 for IgG2c) for a total of 50μL/well, and the plate was incubated for 1 hour at 37°C. After washing the plate four times with wash buffer, secondary antibodies conjugated with HRP (goat anti-mouse IgG-HRP, goat anti-mouse-IgG1-HRP or goat anti-mouse IgG2c-HRP, Southern Biotechnologies Associates) were diluted 1:20,000 in blocking buffer (50μL/well) and was incubated for 30

minutes at 37°C. Once again, the plate was washed six times with wash buffer, and 50µL/well of TMB (3,3',5,5'-tetramethylbenzidine, Millipore) was added. The plates were covered in foil and incubated for 15 minutes at 37°C. Finally, the reaction was stopped by adding 25µL/well of 0.5M H_2SO_4 (Sigma-Aldrich). The plates were immediately read at 450nm, and antibody concentrations were analyzed with respect to the standard curves.

3.1.8 Mice splenocyte isolation and IFN-γ & IL-4 cytokine quantification via sandwich ELISA

For the immunogenicity study, the spleens of all mice were collected during sacrifice at week 10. The spleens were homogenized using a syringe plunger and cell strainer in hank's balanced salt solution (HBSS, Wisent Bioproducts). 0.5mL of splenocytes in HBSS was saved from each mouse injected with BCG and 100µL was plated on 7H11/OADC (containing PANTA: polymyxin-B, amphotericin-B, nalidixic acid, trimethoprim, azilocillin, Thermofisher) for 4 weeks at 37°C to verify the presence of BCG in the spleens. The remainder of the splenocytes in HBSS were then centrifuged at 400rcf for 10 minutes at 4°C [139, 140]. Subsequently, the red blood cells were lysed by resuspending the samples in 3mL of ammonium chloride potassium (ACK) for 3 minutes and HBSS was added to stop the reaction. The spinning and decanting steps were repeated with HBSS two times, then the cells were resuspended in 900uL of complete RPMI media (RPMI-1640, 10% fetal bovine serum, 1mM penicillin/streptomycin, 1X MEM non-essential amino acids, 1mM sodium pyruvate, 1mM L-glutamine, 10mM HEPES, & 0.05 mM 2-mercaptoethanol) (Wisent Bioproducts) [139-141]. Next, trypan blue was mixed with an aliquot of each splenocyte mixture for counting on a haemocytometer, and then the cells were diluted to add $1x10^6$cells/well (100µL/well) to a 96-well U-bottom plate (Greiner Bio-One). Finally, 2.5µg/mL (100µL/well) of purified *Sm*CB protein was added to stimulate cells. The cells were incubated with both 300,000

and 1,000,000 cells at 37°C and 5% CO_2 for 72 hours. The plates were then centrifuged (10,000 rcf for 8 minutes) and the supernatant was collected and stored at -80°C until analyzed via sandwich ELISA for IFN-γ and IL-4 [140].

The splenocytes were later thawed, and the presence of IFN-γ and IL-4 was measured using a sandwich ELISA kit (R&D Systems: Mouse IL-4 or IFN-γ DuoSet ELISA) for each specific cytokine. All incubation steps were conducted at room temperature and used materials and protocols from R&D systems. Firstly, both IFN-γ and IL-4 96 well flat-bottomed ELISA plates were coated with 100µL/well of capture antibody (4.00µg/mL) and incubated overnight (R&D systems). The following day, the plates were washed with 400µL/well wash buffer (pH: 7.4: 0.05% Tween20 in PBS) and blocked with 300µL/well reagent diluent (pH:7.4 0.1% BSA & 0.05% Tween20 in TBS [20mM Trizma base, 150mM NaCl] for IFN-γ, pH: 7.4 1% BSA in PBS for IL-4) for one hour. Next the plates were washed and 100µL/well of 1:10 diluted splenocyte supernatants or standard were added and incubated for two hours. The plates were washed and 100µL/well of detection antibody (250ng/mL) was added and the plates were incubated for two hours. Subsequently, the plates were washed and 100µL/well of Streptavidin-HRP was added and incubated for 20 minutes. Next 100µL/well of substrate solution (TMB) was added and incubated for 20 minutes. Finally, the reaction was stopped by adding 50µL/well of stop solution ($1MH_2SO_4$). The plates were both read immediately at 450nm and cytokine concentrations were analyzed with respect to the standard curves.

3.2 Results

In order to analyze the potential effects of the BCG + *Sm*CB vaccine candidate, two independent mice studies were conducted (Table 2). The 10-week immunogenicity study contained 24 mice in six groups all receiving a two-dose schedule 6 weeks apart, followed by a sacrifice at week 10 to collect the spleens. The IFN-γ, IL-4 cytokine levels, and BCG presence for groups inoculated with BCG, were analyzed from the spleen. The 17-week challenge study contained 20 mice in 4 groups (the two AddaVax groups had to be removed to allow all mice to be challenged at the same time) receiving a two-dose schedule 6 weeks apart, followed by *S. mansoni* challenge at week 10, and sacrifice to measure worm, intestinal and hepatic egg burdens at week 17. The total IgG, IgG1 and IgG2c titers were collected throughout both independent experiments by saphenous blood collection. The IP route was chosen as route of administration, as it is one of the two most commonly used routes for administering BCG in lab studies. Indeed, when comparing multiple routes of administration (intravenous, sub-cutaneous, and intranasal), rBCG expressing a *S. mansoni* glutathione S-transferase (Sm28GST) given IP to mice led to one of the highest antibody responses against the Sm28GST protein [142]. Additionally, a rBCG expressing a *S. mansoni* fatty-acid-binding protein (Sm14) given to mice IP, with various prime-boost schedules, led to 48% reduction in worm burden 4 weeks after challenge [109]. The previously described *S. mansoni* vaccines using *Sm*CB as an antigen combined with either Montanide, CpG, *Salmonella*-vector, AddaVax, or Adenovirus, all used the intramuscular (IM) route and gave 20μg of *Sm*CB at weeks 0, 3 and 6. The IM route could not be repeated for BCG as it may lead to granuloma formation at the site of injection [143]. Furthermore, injections were only given at weeks 0 and 6, since it normally takes 4-8 weeks for BCG to mount cellular and humoral immune responses, and BCG is usually only given once (as a prime) [144, 145].

Table 2. Immunogenicity and Challenge study mice groups. All inoculations were diluted in PBS-Tween80-0.05%. All mice were injected with 450µL of vaccine formulation IP. The sacrifice for the immunogenicity study includes collection of spleens, while the sacrifice for the challenge study includes collecting worms from the portal venous system, as well as intestine and liver to measure egg burden. The challenge includes infecting mice with 150 *S. mansoni* cercariae (Puerto Rican strain) shed from *Biomphalaria glabrata* infected snails.

	# of mice	Antigen	Adjuvant	Week 0	Week 6	Week 10	Week 17
Immunogenicity:							
PBS	**3**	**N/A**	**N/A**	**Dose 1**	**Dose 2**	**Sacrifice**	**N/A**
BCG + *Sm*CB	**4**	***Sm*CB (20µg)**	**BCG-Danish (1.00 x 10^6 CFU)**	**Dose 1**	**Dose 2**	**Sacrifice**	**N/A**
BCG	**5**	**N/A**	**BCG-Danish (1.00 x 10^6 CFU)**	**Dose 1**	**Dose 2**	**Sacrifice**	**N/A**
***Sm*CB**	**4**	***Sm*CB (20µg)**	**N/A**	**Dose 1**	**Dose 2**	**Sacrifice**	**N/A**
AddaVax	**3**	**N/A**	**AddaVax (25µL)**	**Dose 1**	**Dose 2**	**Sacrifice**	**N/A**
AddaVax + *Sm*CB	**5**	***Sm*CB (20µg)**	**AddaVax (25µL)**	**Dose 1**	**Dose 2**	**Sacrifice**	**N/A**
Challenge:							
PBS	**5**	**N/A**	**N/A**	**Dose 1**	**Dose 2**	**Challenge**	**Sacrifice**
BCG + *Sm*CB	**5**	***Sm*CB (20µg)**	**BCG-Danish (1.00 x 10^6 CFU)**	**Dose 1**	**Dose 2**	**Challenge**	**Sacrifice**
BCG	**5**	**N/A**	**BCG-Danish (1.00 x 10^6 CFU)**	**Dose 1**	**Dose 2**	**Challenge**	**Sacrifice**
***Sm*CB**	**5**	***Sm*CB (20µg)**	**N/A**	**Dose 1**	**Dose 2**	**Challenge**	**Sacrifice**

3.2.1 Schistosoma mansoni challenge and protection from infection post-immunization

As previously mentioned, the protective efficacy of each vaccine group was measured by inoculating mice with a two-dose schedule 6 weeks apart (Table 2). All mice survived to the day of sacrifice (20 mice in total, 5 mice per group). The worms and eggs collected from the vaccine groups were counted and compared to the PBS group to calculate parasitic reduction percentages using the previously described equation (3.1.3). The results were then analyzed using the Kruskal Wallis one-way ANOVA with Dunn's multiple comparison tests (GraphPad Prism 9). This analysis used a non-parametric approach to measure the difference between the means of all the vaccine groups and to determine statistical significance [146]. The PBS group contained an average of 39 ± 3 worms per mouse. All groups reduced the number of worms compared to the PBS control with a mean reduction of 44.9% ± 6.5% for BCG+ *Sm*CB, 48.5% ± 12.5% for BCG alone, & 41.4% ± 6.7% for purified *Sm*CB alone (Figure 6A). The BCG alone group had the highest mean worm reduction (48.5%) however it also contained a larger standard error (±12.5%), which is why through ANOVA (which takes into account standard deviation discrepancies between groups), it was not a statistically significant reduction compared to the PBS group. Only the BCG + *Sm*CB formulation significantly reduced the number of worms, with respect to the PBS group, with a mean reduction of 44.9% ± 6.5% (p value of < 0.05). The PBS group also contained intestinal eggs, ranging from 6,487 to 20,075 eggs/gram intestine. The vaccine groups reduced the number of intestinal eggs relative to PBS by 35.8% ± 7.4% for BCG + *Sm*CB, 13.5% ± 6.3% for BCG, & 23.5% ± 8.4% for *Sm*CB (Figure 6B). Once again, only the BCG + *Sm*CB group significantly reduced the number of intestinal eggs, with respect to the PBS group, with the highest mean of the three formulations, a reduction of 35.8% ± 7.4%, and a p value of < 0.05. Finally, the PBS group contained hepatic eggs ranging from 5,457 to 12,065 eggs/gram liver tissue. Hepatic

egg reduction in the groups compared to PBS were 20.0% ± 7.1% for BCG+ *Sm*CB, 16.3% ± 9.8% for BCG, & 5.4% ± 4.9% *Sm*CB (Figure 6C). Although all groups reduced the number of hepatic eggs, none were statistically significant. However, the BCG+ *Sm*CB formulation had the highest level of reduction (20.0% ± 7.1%). Note that there were no statistical differences in burdens between the three individual formulations for either worms or eggs. However, taken together, the data herein indicate that the BCG + *Sm*CB vaccine formulation was superior in reducing the burden of worms as well as eggs in both the intestines and liver.

A

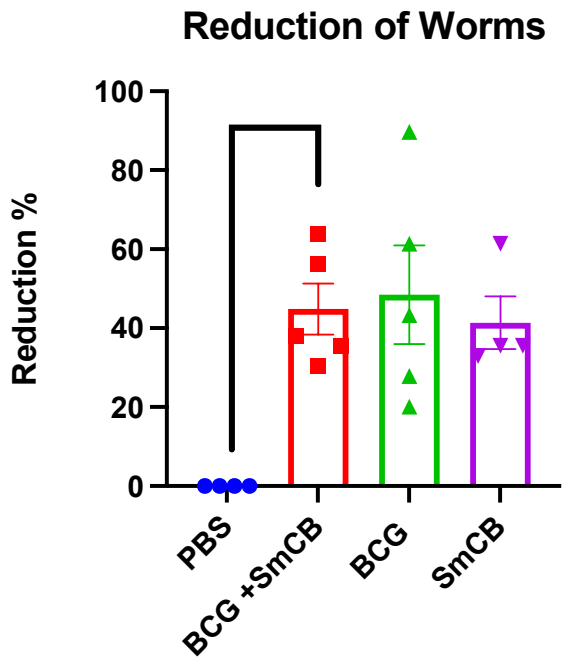

B

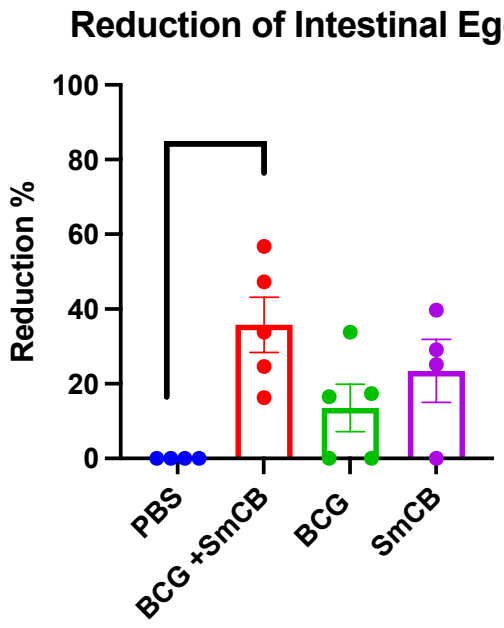

C

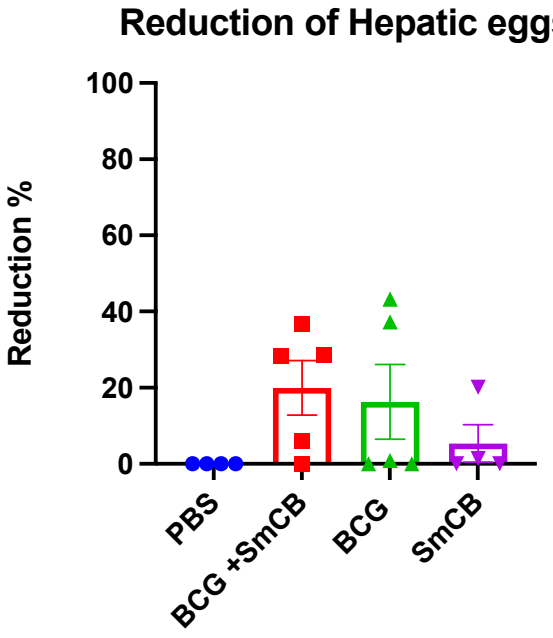

Figure 6: Parasite egg and worm burden. The mean reduction percentage, along with SEM, was graphed for each group relative to the PBS control group (represented by the column bars). Each mouse is graphed as an individual dot. Worm burden in the portal venous system **(6A)** intestinal egg reduction **(6B)** and hepatic egg reduction **(6C)**. Statistical significance was only observed for the BCG+ *Sm*CB group against the PBS control group **(6A & 6B)**. Means and SEM are shown. n = 5 per group, *P < 0.05.

3.2.2 Humoral response by indirect ELISA

Since the BCG + *Sm*CB vaccine formulation demonstrated significant protective efficacy towards both *S. mansoni* worms and intestinal eggs, the specific humoral responses involved in these protective effects were analyzed. As previously mentioned, a two-dose schedule 6 weeks apart was given to each mouse IP. The mice in the immunogenicity study were sacrificed at week 10, while the challenge mice were challenged at week 10, and sacrificed at week 17 (Figure 7). Mouse sera were collected through saphenous bleeds at weeks 0, 6 and 10 for both studies, as well as week 12, 14 and 17 for the challenge study. The immunogenicity study contained 24 mice total, and the challenge study contained 20 mice total, whereby the AddaVax + *Sm*CB group was removed from the latter study as the maximum number of animals that could be infected at any one time was 20. For all *Sm*CB-specific total IgG, IgG1 and IgG2c indirect ELISA analyses, the mice data from both studies were pooled from week 0 to week 10, while week 12 onwards only contains data from the challenge study (Figure 7, Figure 8). Similarly, to the analysis of vaccine efficacy, all results were analyzed using the Kruskal Wallis one-way ANOVA with Dunn's multiple comparison tests to measure the difference between the means of all the vaccine groups and determine statistical significance (GraphPad Prism 9).

Beginning with the analysis of total IgG, at baseline there was little to no detectable *Sm*CB-specific IgG (*Sm*CB-IgG), and vaccine groups from both studies were similar (Figure 8A). Six weeks after the first injection, the AddaVax + *Sm*CB (mean of 1347 ± 253 ng/mL) and BCG + *Sm*CB (795.8 ± 221 ng/mL) groups developed *Sm*CB-IgG responses, where the AddaVax + *Sm*CB group had the highest response, while the other four groups remained similar to baseline. There were still no statistically significant differences between any of the groups. By week 10, four weeks after the second injection, both the BCG + *Sm*CB (5111 ± 925 ng/mL) and AddaVax + *Sm*CB

(4627 ± 858ng/mL) formulations had significantly increased *Sm*CB-IgG responses (Figure 7A, Figure 8A). The BCG + *Sm*CB group showed significantly increased *Sm*CB-IgG with respect to the *Sm*CB (*P < 0.05), BCG (**P < 0.01) and PBS (***P < 0.001) groups, while the AddaVax + *Sm*CB group had significantly increased levels of *Sm*CB-IgG with respect to the BCG (*P < 0.05) and PBS (*P < 0.05) groups.

For week 12 (2 weeks post-challenge), now focusing solely on the four groups from the challenge study, there was a slight reduction of *Sm*CB-IgG in the *Sm*CB, BCG & PBS groups, however the BCG + *Sm*CB (6414 ± 2058 ng/mL) group had a slight increase of *Sm*CB-IgG responses from week 10 (Figure 8A). At week 12 the BCG + *Sm*CB group maintained a significant increase in *Sm*CB-IgG responses with respect to the *Sm*CB and PBS groups (both *P < 0.05). However, by week 14, there was a reduction of *Sm*CB-IgG responses in the BCG + *Sm*CB (2577 ± 621.6 ng/mL) group, but there was still statistical significance between BCG + *Sm*CB with respect to both *Sm*CB (*P < 0.05) and PBS (**P < 0.01) (Figure 8A). Additionally at week 14, *Sm*CB-IgG in the control groups (*Sm*CB, BCG & PBS) remained low, comparable to week 12. Finally at week 17, when the challenge mice were sacrificed, the BCG + *Sm*CB (9800 ± 2060 ng/mL) formulation had significantly increased *Sm*CB-IgG responses to the highest level detected and demonstrated statistical significance with respect to the *Sm*CB group (**P < 0.01). It is also important to note that all four groups had the highest detected amount of *Sm*CB-IgG responses at this time point (PBS = 1965 ± 167 ng/mL, BCG = 2051 ± 340 ng/mL, *Sm*CB = 1283 ± 240 ng/mL) most likely due to the mice's natural immune response to the *cathepsin B* contained in the *S. mansoni* worms and eggs (Figure 7B, Figure 8A).

Since the total IgG humoral response to infection was analyzed for all vaccine groups, the IgG subclasses were also analyzed to discover which specific Th2 (IgG1) or Th1 (IgG2c) derived antibody responses have the most influence from the vaccines and *S. mansoni* infection. Starting with Th2 derived IgG1, at week 0 there was little to no detectable *Sm*CB-specific IgG1 (*Sm*CB-IgG1) for all mice (Figure 8B). Six weeks after the first injection, the AddaVax + *Sm*CB (mean of 331.8 ± 56 ng/mL) developed a very slight *Sm*CB-IgG1 response, while all the other groups remained similar to baseline. There were still no statistically significant differences between any of the groups at this point. At week 10, four weeks after the second injection, AddaVax + *Sm*CB (mean of 1618 ± 409 ng/mL) was the sole group that developed a statistically significant *Sm*CB-IgG1 response with respect to the BCG (*$P < 0.05$), AddaVax (**$P < 0.01$), and PBS (**$P < 0.01$) groups (Figure 8B). However, BCG + *Sm*CB (556 ± 149 ng/mL) followed by *Sm*CB (303 ± 99 ng/mL) both developed a slight increase in *Sm*CB-IgG1 response compared to the other groups that remained close to baseline (BCG, AddaVax & PBS). For both week 12 and 14 (2- and 4-weeks post infection), the *Sm*CB-IgG1 responses in all four groups dropped to baseline (Figure 8B). However, similarly to what was observed for total *Sm*CB-IgG, by week 17 the *Sm*CB-IgG1 responses in all four groups reached their maximum *Sm*CB-IgG1 response in the following order: PBS (1989 ± 1488 ng/mL), BCG + *Sm*CB (1067 ± 455 ng/mL), BCG (805 ± 149ng/mL) then *Sm*CB (590 ± 169 ng/mL) (Figure 8B). Although it is important to note that there was a very large variance between the mice within each group, hence the large standard error of mean, particularly for the PBS group which contained one mouse that reached a *Sm*CB-IgG1 response of 7934 ng/mL. This week 17 ELISA time point was repeated to ensure that no errors were made, and the same concentrations were observed for all the mice. Ultimately, weeks 12, 14 and 17, demonstrated no statistical significance between the four vaccine groups.

Considering that all mouse vaccine groups produced similar trends for *Sm*CB-specific total IgG and IgG1 immune responses over time, IgG2c was next analyzed to determine the effects of Th1 derived antibody responses. Between IgG2a, IgG2b and IgG2c, the latter was chosen due to its use in previous *Sm*CB vaccine studies, as well as a recent study in C57BL/6 mice which concluded that the most correct analysis of Th1 responses (for a *Plasmodium vivax* TRAP subunit vaccine) was done by measuring IgG2c (instead of IgG2a) along with IFN-γ[147]. Unfortunately, sufficient mouse sera from weeks 6, 12, and 14 were not available to be analyzed. Therefore, *Sm*CB-specific IgG2c (*Sm*CB-IgG2c) was only analyzed for weeks 0 and 10 (pooled mice data from both studies) and week 17 (challenge study). Starting with week 0, all six groups had low amounts of *Sm*CB-IgG2c, relatively close to baseline (Figure 8C). At week 10, four weeks after the second injection, BCG + *Sm*CB (mean of 601 ± 50 ng/mL) was the only group that developed a statistically significant *Sm*CB-IgG2c response with respect to the *Sm*CB and PBS groups (both $*P < 0.05$) (Figure 8C). Moreover, the AddaVax + *Sm*CB group had little to no detectable *Sm*CB-IgG2c responses, which is very different from the high *Sm*CB-IgG and *Sm*CB-IgG1 responses observed previously at week 10 (Figure 7, Figure 8). Week 17 was comparable to week 10 where BCG + *Sm*CB (mean of 1949 ± 900 ng/mL) was the only group that developed a statistically significant *Sm*CB-IgG2c response with respect to the *Sm*CB and BCG groups (both $*P < 0.05$) (Figure 8C).

In conclusion, although both BCG + *Sm*CB and AddaVax + *Sm*CB developed statistically significant *Sm*CB-specific total IgG and IgG1 humoral responses, the BCG + *Sm*CB formulation developed a more observable mixed IgG1/IgG2c response (Figure 8). However, the AddaVax + *Sm*CB formulation seemed to generate slightly earlier significant *Sm*CB-specific total IgG and

IgG1 response (since it had higher titers at week 6), and it had a much higher *Sm*CB-IgG1 response at week 10 (Figure 8). Alternatively, the BCG + *Sm*CB formulation generated a higher *Sm*CB-IgG2c response at week 10 compared to AddaVax + *Sm*CB (which did not generate an observable *Sm*CB-IgG2c response). Therefore, the BCG+ *Sm*CB formulation seems to favor a more Th1 dependent humoral response, while the AddaVax + *Sm*CB formulation favored a more Th2 dependent humoral response, which is expected. Moreover, the mean amount of total *Sm*CB-specific total IgG was quite similar between the BCG + *Sm*CB and AddaVax + *Sm*CB formulations, although the significance of the BCG + *Sm*CB group was higher (***$P < 0.001$ versus *$P < 0.05$ respectively) since it had a much smaller standard error (Figure 7). Finally, it is important to note that the statical significance observed were not only relative to the PBS group, but relative to the other control groups as well, including the *Sm*CB, AddaVax, and BCG groups. The latter is due to the wide range for baseline when using the ELISA protocol (baseline ranging from approximately 0 to 400 ng/mL) and is further discussed in the discussion.

A

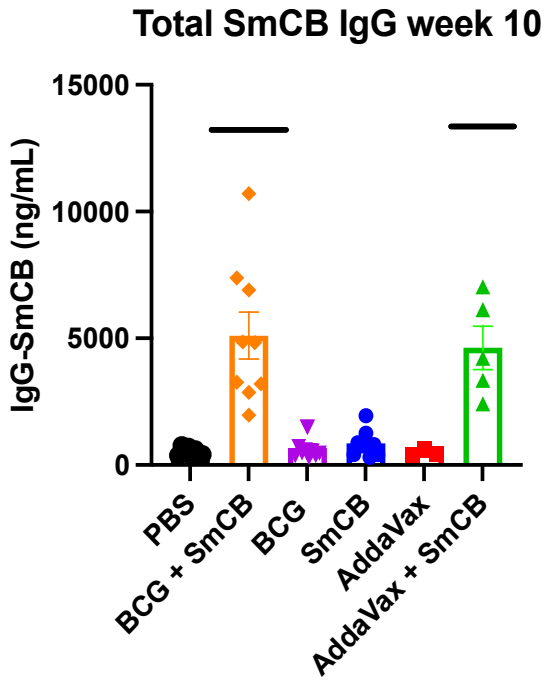

B

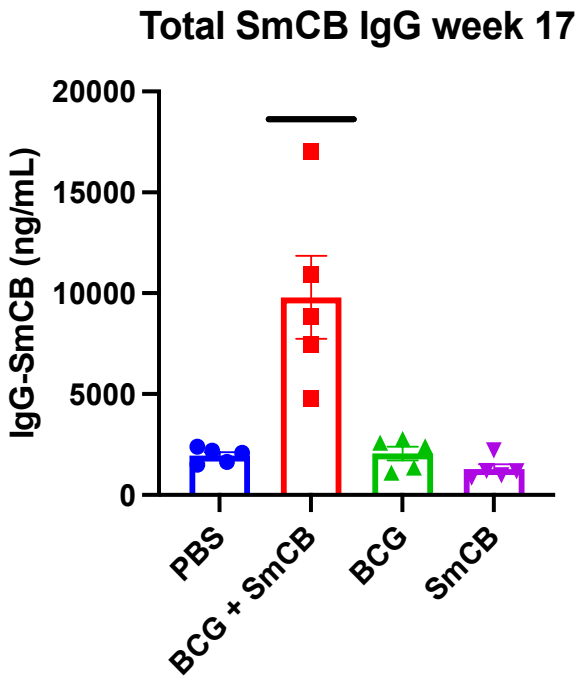

Figure 7: Humoral response: endpoint *Sm*CB IgG titers from immunogenicity and challenge study. The mean concentration of *Sm*CB IgG, along with SEM (represented by the column bars), was graphed for all groups in the immunogenicity (n = 24 total, PBS: n = 3, BCG + *Sm*CB n = 4, BCG n = 5, *Sm*CB n = 4, AddaVax n = 3, AddaVax + *Sm*CB n = 5) and challenge study (n = 20 total, n = 5 for each group). Each mouse is graphed as an individual dot. **7A:** For week 10, the titers were pooled from both the immunogenicity and challenge studies, n= 44. At week 10, the BCG + *Sm*CB formulation had significantly increased *Sm*CB specific IgG with respect to the *Sm*CB (*P < 0.05), BCG (**P < 0.01) and PBS (***P < 0.001) groups, while the AddaVax + *Sm*CB group had significantly increased *Sm*CB specific IgG with respect to the BCG (*P < 0.05) and PBS (*P < 0.05) groups. **7B:** For week 17 (7 weeks post-challenge), the BCG + *Sm*CB formulation significantly increased *Sm*CB specific IgG with respect to the *Sm*CB group (**P < 0.01). Serum from individual mice was analyzed by ELISA. *P < 0.05, **P < 0.01, ***P < 0.001.

A

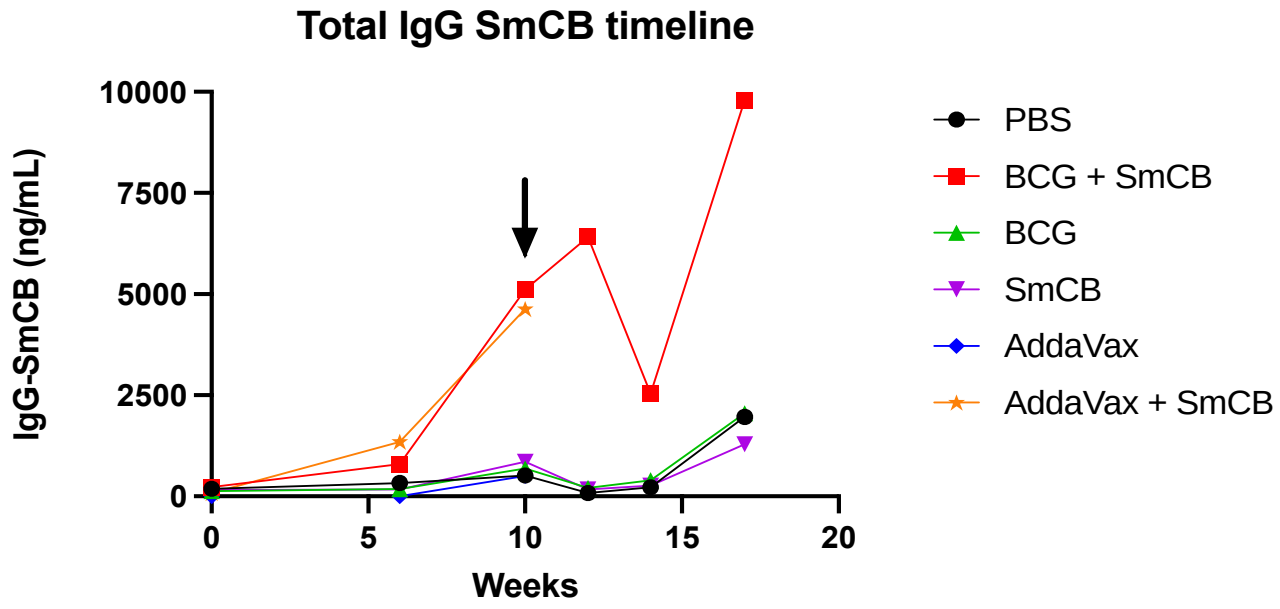

B

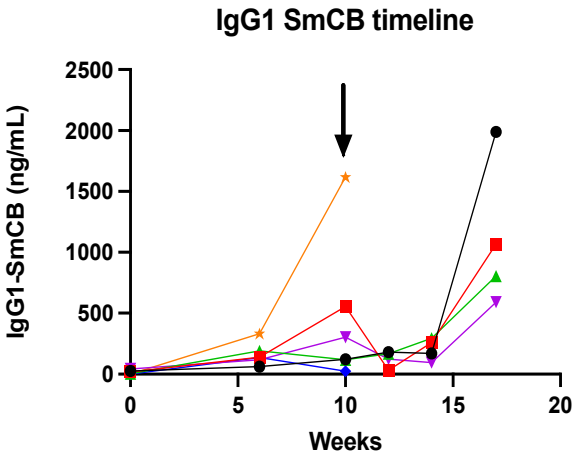

C

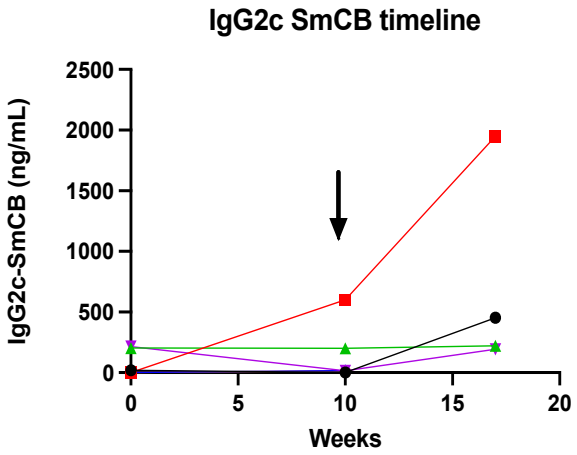

Figure 8: Humoral response: *Sm*CB specific total IgG, IgG1 & IgG2c titers over time. The mean concentration of *Sm*CB specific total IgG **(A)**, IgG1 **(B)**, and IgG2c **(C)** are graphed from different time points. For all timelines, mice sera from both the immunogenicity (n = 24 total, PBS: n = 3, BCG + *Sm*CB n = 4, BCG n = 5, *Sm*CB n = 4, AddaVax n = 3, AddaVax + *Sm*CB n = 5), and challenge (n = 20 total, n = 5 for each group) studies were pooled from week 0 to week 10 (n = 44). The black arrow indicates when the immunogenicity mice were sacrificed and when the challenge mice were infected with *S. mansoni* cercariae. **8A:** For *Sm*CB total IgG, mice sera from weeks 0, 6, 10, 12, 14 and 17 were analyzed. Statistical significance between groups at weeks 10 and 17 are in Figure 7A. The BCG + *Sm*CB group demonstrated statistical significance compared to *Sm*CB and PBS at weeks 12 and 14. **8B:** For *Sm*CB IgG1, mice sera from weeks 0, 6, 10, 12, 14 and 17 were analyzed. The AddaVax + *Sm*CB group demonstrated statistical significance compared to AddaVax, BCG and PBS at week 10. **8C:** For *Sm*CB IgG2c, mice sera from weeks 0, 6 and 17 were analyzed. The BCG + *Sm*CB group demonstrated statistical significance compared to the *Sm*CB and PBS groups at week 10, and the *Sm*CB and BCG groups at week 17. The AddaVax and AddaVax + *Sm*CB are graphed but difficult to see since they are close to baseline. Serum from individual mice was analyzed by ELISA.

3.2.3 Mice splenocyte isolation and IFN-γ & IL-4 cytokine production via sandwich ELISA

As previously mentioned in the immunogenicity study, mice inoculated with BCG needed further confirmation that BCG remained viable throughout the experiment to prove that the immunological effects observed were from the presence of live BCG. The BCG counts in the spleen were analyzed by plating 100µL of spleen/HBSS on 7H11/OADC/PANTA at 4 weeks at 37°C for all mice injected with BCG. After colony counting, a substantial amount of BCG bacteria was found in all mice, with a range from 5.1 x 10^3 to 21.5 x 10^3 CFU/spleen, and an average of 14.0 x 10^3 CFU/spleen. The average amount of BCG bacteria was slightly higher in the mice injected with BCG+ *Sm*CB (15.2 x 10^3 CFU/spleen) compared to those injected with BCG (13.0 x 10^3 CFU/spleen). BCG presence in organs after one injection has been shown to decrease from 2 weeks to 16 weeks after injection, where by 16 weeks the bacteria is eliminated (or below the limit of detection) [142]. Therefore, since viable BCG was recovered in the spleen 4 weeks after the second injection, protective efficacy (through cellular and humoral immunity) may be enhanced due to the presence of BCG [148]. This was explored as described in the following section.

After observing the protective efficacy (through worm and egg reduction) and humoral responses (through *Sm*CB-specific IgG, IgG1 & IgG2c) of each vaccine formulation over time, the cell-mediated immune responses from the spleen were then analyzed to further explore the immune mechanisms of each vaccine. To verify splenic cell-mediated immune responses, the signature IFN-γ & IL-4 cytokines were chosen to detect Th1 and Th2-type mediated responses respectively [149]. As previously mentioned in the materials and methods, splenocytes were obtained from the week 10 sacrifice of the immunogenicity study, containing 24 mice in total from 6 different vaccine groups.. For both cytokines, a sandwich ELISA method was chosen as it is approximately 2-5

times more sensitive than direct or indirect ELISA, and it offers high specificity since two antibodies (which detect different epitopes) are used for antigen detection [150]. Similar to the analysis of vaccine efficacy, and the humoral responses, all results were analyzed using the Kruskal Wallis one-way ANOVA with Dunn's multiple comparison tests to measure the difference between the means of all the vaccine groups and determine statistical significance (GraphPad Prism 9).

Beginning with IFN-γ, this pro-inflammatory cytokine has a vital role in activating Th1 cells and macrophages, as well as upregulating MHC class I expression and antigen presentation on cells [151, 152]. Moreover, since BCG is known to activate strong Th1 responses, IFN-γ present in mice splenocytes stimulated with *Sm*CB can be analyzed to see if the BCG vaccine groups demonstrate an enhanced production of this cytokine [153]. The AddaVax + *Sm*CB vaccine formulation produced the highest amount of IFN-γ (mean of 5022 ± 1306 pg/mL) followed by BCG+ *Sm*CB (3262 ± 1384pg/mL), BCG (2949 ± 309 pg/mL), *Sm*CB (2616 ± 323 pg/mL), PBS (2473 ± 225 pg/mL), then AddaVax (1593 ± 653 pg/mL) (Figure 9A). However, it is important to note that there was no statistical significance between any of the groups, partially due to the very large variance between the mice within each group. Specifically, the standard error of mean for the AddaVax + *Sm*CB and BCG+ *Sm*CB vaccine formulations were the largest. Moreover, the amount of IFN-γ in the control groups, specifically PBS and AddaVax, was very high. The latter may have occurred due to impurities in the original BSA that was used as both a reagent diluent and blocking buffer during the assay. The R&D systems handbook indicated that even very slight impurities can lead to over-detection at background [154]. Therefore, for the IL-4 assay, new BSA

specifically designed for use in this sandwich ELISA was used, but the IFN-γ experiment could unfortunately not be repeated due to a lack of usable supernatant.

The IL-4 cytokine is representative of a Th2 response, which is associated with protection against helminth infections, and more importantly essential to host survival in the case of *S. mansoni* [155]. Moreover, AddaVax, similar in composition to MF59, elicits both Th1 and Th2 responses, with a slight Th2 bias [156, 157]. Therefore, analyzing the IL-4 present in mice splenocytes stimulated with *Sm*CB can be used to examine differences between the AddaVax and other vaccine groups. Contrary to what was expected, the AddaVax groups (AddaVax 87 ± 45 pg/mL, AddaVax + *Sm*CB 28 ± 27 pg/mL) had the lowest amount of detected IL-4, while the BCG+ *Sm*CB (271 ± 128 pg/mL) group had the highest (Figure 9B). The PBS (94 ± 46 pg/mL) and BCG (82 ± 33 pg/mL) groups were close to one another, followed by *Sm*CB (0 pg/mL) which had no IL-4 detected. However, it is important to note that all levels of IL-4 detected were very low in all groups, and the variance was very large between mice within the same group. The latter is mainly due to difficulty in detecting differences in concentration at such low levels [158]. Moreover, there was no statistical significance in between any of the groups.

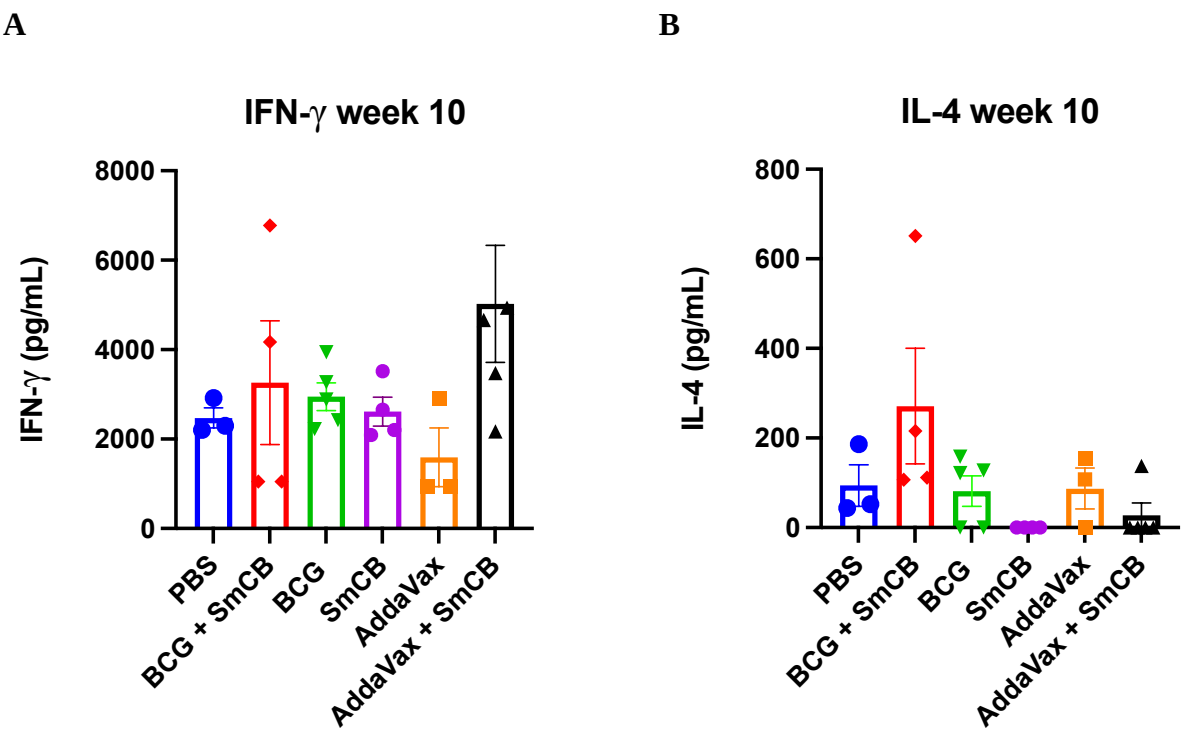

Figure 9: Cellular immune response: IFN-γ and IL-4 cytokine production at week 10. The mean concentration of IFN-γ **(9A)** and IL-4 **(9B)**, along with SEM (represented by the column bars), was graphed for all groups in the immunogenicity study (n = 24 total, PBS: n = 3, BCG + *Sm*CB n = 4, BCG n = 5, *Sm*CB n = 4, AddaVax n = 3, AddaVax + *Sm*CB n = 5). Each mouse is graphed as an individual dot. **9A:** The AddaVax + *Sm*CB group demonstrated the highest amount of IFN-γ, followed by BCG + *Sm*CB. **9B:** The BCG + *Sm*CB group demonstrated the highest amount of IL-4. Statistical significance was not observed between any groups. Splenocytes stimulated with *Sm*CB from individual mice were analyzed by sandwich ELISA.

3.3 Discussion

This pilot study co-administering the previously studied *Sm*CB with BCG peritoneally into C57BL/6 mice 0 and 6 weeks apart, is a novel experimental approach towards discovering a Schistosomiasis vaccine. As previously mentioned, if a vaccine elicits both humoral and cellular immunity towards *Sm*CB, and protection against *S. mansoni* infection, then it may be a successful vaccine candidate for Schistosomiasis. Furthermore, in the study described herein, the protective efficacy for the BCG + *Sm*CB vaccine reached 45%, which is above the 40% threshold set by the WHO [18]. As such, already after the first attempt, the BCG + *Sm*CB vaccine formulation shows strong potential for being a successful vaccination strategy and certainly warrants further investigation and repeated studies in the future.

Beginning with protective efficacy against *S. mansoni* cercarial challenge, the protective efficacy was only analyzed for four groups, specifically BCG + *Sm*CB, *Sm*CB, BCG & PBS, but not AddaVax, and AddaVax + *Sm*CB. Comparing the reduction in worms and eggs to an AddaVax + *Sm*CB formulation IP would be beneficial since previous studies using AddaVax and *Sm*CB reached protective rates of up to 86.8% when following an IM three dose schedule [137]. This comparison would also be insightful for cell-mediated responses, specifically since BCG should enhance Th1 responses, while AddaVax should provide a mixed Th1/Th2 response with a slight Th2 bias [153, 156]. Although the BCG+ *Sm*CB vaccine induced a significant reduction in worms and intestinal eggs, the reduction in the hepatic eggs was not significant. This is interesting since in the challenge study the livers from the mice inoculated with either BCG or BCG + *Sm*CB had severe liver pathology (data not shown), which has been previously observed in *S. mansoni* infected mice that demonstrated high Th1 polarized responses [137]. This aligns with the

immunogenicity study that demonstrated that the BCG bacteria from the vaccines proliferated in the spleen, and most likely other organs, thereby inducing non-specific inflammatory responses as well as *Sm*CB specific Th1 responses in the case of the BCG +*Sm*CB vaccine [95]. Therefore, the expression of Th1 pro-inflammatory cytokines induced by the BCG vaccines may be contributing to deleterious liver pathology. Furthermore, although not statistically significant, it is important to note that the BCG alone and *Sm*CB alone vaccine formulations all demonstrated worm, intestinal and hepatic egg reductions. This may be supporting evidence of BCG's non-specific immunomodulatory effects, as well as the potential of targeting the *Sm*CB antigen for future vaccine candidates, since it may induce protective immune responses against challenge alone[95].

Furthermore, in the challenge study, an interesting observation in total IgG and IgG1 was observed between weeks 12 and 14 (2- and 4-weeks post-challenge) where a dip in these two antibody titers was detected in all groups, and was particularly pronounced for the BCG+*Sm*CB group (Figure 8). More specifically focusing on the BCG+ *Sm*CB formulation, an increase in *Sm*CB-IgG was observed from week 10 to week 12, then a significant drop occurred by week 14, followed by a rise to the highest *Sm*CB-IgG observed at week 17. Moreover, for the *Sm*CB-IgG1 antibody, a slightly different trend was observed where titers dropped at week 10, stayed low until week 14 then rose once again to the highest *Sm*CB-IgG1 level detected at week 17. Previous vaccine studies using *Sm*CB have looked at week 10 and 17 IgG, IgG1 & IgG2c titers, but not weeks 12 and 14. Studies analyzing antibody responses post-infection with *S. japonicum* in mice have demonstrated that specific IgG responses usually first appear 2 weeks after infection, but do not reach a positive threshold until over 4 weeks post-infection[159]. Furthermore, *S. mansoni* infection is known to induce a Th1 response against the cercariae, schistosomes and adult worms

during the first 6 weeks of infection, followed by the induction of regulatory T cells leading to a Th2 skewed response against the eggs approximately 7 to 12 weeks after infection, with a peak Th2 response close to week 9 [160]. As per Fig. 8B, we observe this rise in the *Sm*CB-specific Th2 response across all groups between weeks 14-17 post-challenge, and it is particularly evident in the unvaccinated (PBS only) mice (1989± 1488 ng/mL), supporting the induction of a Th2 response against the parasite eggs. Although not challenged, the AddaVax + *Sm*CB group showed the highest Th2-associated IgG1 response beyond week 6. The initial Th1 response to the BCG + *Sm*CB vaccine may be responsible for the drop in *Sm*CB-IgG1 for weeks 12 and 14, and egg deposition could have induced the rise of *Sm*CB-IgG1 by week 17. Unfortunately, the *Sm*CB-IgG2c antibody titers could not be observed at weeks 12 and 14 to see if they increased while IgG1 decreased. However, at week 17, the *Sm*CB-IgG2c (1949 ± 900 ng/mL) titers were still higher than *Sm*CB-IgG1 (1067 ± 455 ng/mL) for the BCG +_*Sm*CB vaccinated animals, consistent with the BCG + *Sm*CB vaccine being Th1 dominant. For the other groups, the response appeared to be dominated by IgG1 by 7 weeks post-challenge (Figure 8B, Figure 8C). The reduction in the IgG1 response in the 3 vaccine groups (BCG, BCG + *Sm*CB & *Sm*CB) compared to the PBS controls, is consistent with the reduced worm and egg burden observed in all the vaccinated groups. Of note, the total *Sm*CB-specific IgG response in the BCG + *Sm*CB vaccinated animals exceeds the combined IgG1 and IgG2c levels from weeks 10-17 by approx. 3-fold, suggesting that additional IgG subtypes are being induced within this group which should be investigated in the future. A similar effect was noted for the AddaVax + *Sm*CB group at week 10, although no IgG2 was detected in this case. Further analysis of Th2 responses could also be done by looking at IgE antibody titers. IgE is known to play an important role in secreting Th2 cytokines, IL-4 and IL-3, through the activation of basophils, mast cells, and antigen presentation [161, 162]. With regards

to schistosomiasis, IgE antibodies have been linked to resistance to re-infection, and these responses have increased with drug treatment and age, supporting its role in acquired immunity [163-165]. However, vaccine induced IgE hypersensitivity is known to cause detrimental effects, so verifying the vaccine formulations for a large increase in IgE may help screen for this type of sensitivity [137, 166, 167]. Finally an increase in Th17 responses could also be interesting to analyze in the vaccine formulations, due to its association with exacerbated egg-induced inflammation in schistosomiasis in mice, and since Th1, Th2, Th17 and Tregs cross-regulate one another during infection [168-171].

As previously mentioned, vaccines which elicit a mixed Th1/Th2 response, along with high protective antibody titers, result in higher levels of protection upon *Schistosoma* challenge in mice [18, 69, 71]. Based on the humoral responses observed in this study, through IgG subclasses, the BCG + *Sm*CB vaccine elicited a statistically significant increase in *Sm*CB-IgG and *Sm*CB-IgG2c titers, and a slight increase in IgG1, which supports the Th1/Th2 mix with a more dominant Th1 antibody response expected from the BCG mixture. On the contrary, the AddaVax+ *Sm*CB formulation provided statistically significant *Sm*CB-IgG and *Sm*CB IgG1, but no detectable IgG2c. Therefore, through just the analysis of IgG subclasses, the BCG + *Sm*CB formulation provided a slightly more mixed Th1/Th2 response, with a slight Th1 bias, while the AddaVax + *Sm*CB provided a more Th2 biased response. For the cellular mediated immunity analyzed using the week 10 splenocytes, the immune responses did not completely align with the humoral responses observed. Since the BCG + *Sm*CB vaccine demonstrated mixed Th1/Th2 antibodies, with Th1 dominance, it would be expected to have significantly high levels of IFN-γ, while the opposite would be expected for AddaVax+ *Sm*CB since it demonstrated more Th2 biased antibodies.

However, this was not observed, as firstly neither BCG + *Sm*CB nor AddaVax+ *Sm*CB vaccine formulations induced a statistically significant increase in either IFN-γ or IL-4 in the unchallenged animals. Secondly, the AddaVax+ *Sm*CB vaccine had a trend toward more IFN-γ than BCG + *Sm*CB, and BCG + *Sm*CB showed a trend toward more IL-4 than AddaVax+ *Sm*CB (Figure 9). These results may indicate that the vaccines do not induce significant *Sm*CB-specific cellular responses, and that the protective efficacy to challenge is more associated with the humoral responses. Alternatively, the analysis of only the IFN-γ and IL-4 cytokines could have been a limitation, and using multiplex ELISA (such as the Quansys 16-plex ELISA kit which analyzes 16 cytokines and chemokines including: IL1-a, IL1-b, IL-2, IL-3, IL-4, IL-5, IL-6, IL-10, IL-12p70, IL-17, IFNy, TNFa, CCL2, CCL3, CSF2 (GM-CSF), and CCL5) would provide more insight into the immunological profile of each vaccine formulation.

The ELISA detection method used in this study did have some limitations that need to be addressed. Firstly, there was a very high level of background observed in both the indirect and sandwich ELISA. This was particularly problematic for the IFN-γ ELISA (Fig. 9A). It has been previously indicated that impurities in BSA can lead to higher background, however the use of the lower ends of the standard curves (where the amounts present in our samples tended to lie) caused some issues as well since the standard curves may be less accurate closer to the lower bounds, making it difficult to detect differences between samples with low concentrations of antibodies or cytokines [172]. The latter is supported by the large range of background observed in control groups, as well as the large standard error within each vaccine group, although some degree of variance commonly occurs between mice within the same experimental vaccine group [150, 173]. In addition, impurities within the purified *Sm*CB protein (expressed in yeast) may also have

contributed to the high background observed for the IFN-γ ELISA as a result of some non-specific pro-inflammatory activity.

In conclusion, the BCG+ *Sm*CB experimental vaccine formulation given to C57BL/6 mice IP at weeks 0 and 6 did demonstrate significant reduction in worms and intestinal eggs potentially due to the significant IgG and IgG2c humoral responses observed, and most likely additional cellular-mediated mechanisms of action that await further testing and confirmation.

Chapter 4: Future Directions

Further future directions for vaccines using *Sm*CB co-administered with BCG, or recombinant BCG-*Sm*CB, vaccine candidates would ideally include generating a fully functional rBCG-*Sm*CB construct in BCG-Danish (with successful detectable protein expression) that could be inoculated in mice. A recombinant BCG vaccine using *Sm*CB could be more immunogenic than co-administering BCG + *Sm*CB, since rBCG could enhance the protection through innate immune cell stimulation and would ensure colocalization of *Sm*CB and BCG over an extended period of time (which is not necessarily the case when simply injecting a mixture of soluble *Sm*CB and BCG bacteria). However, this novel study did help support the feasibility that BCG could be used in *Schistosomiasis* vaccine development [174]. Additionally, repeating the studies to find the optimal route of administration, dose schedule, and ratio of BCG-*Sm*CB, would certainly increase immunogenicity. The amount of *Sm*CB given to each mouse (20μg) and the original dose schedule IM was optimized for previous vaccine studies using *Sm*CB with either Montanide, CpG, *Salmonella*-vector, AddaVax, and Adenovirus [42, 69, 88, 137, 175]. Therefore, optimizing these factors for BCG would be required as well. In addition, the C57BL/6 mice used for this study are Th1 dominant, meaning they have high IFN-γ and low IL-4, which could also explain why the IL-4 levels observed were very low [135]. Using different mice breeds such as BALB/c mice, which prefer Th2 cytokine, or out-bred mice could also help investigate the generalizability of the vaccine [135, 176]. Also the laboratory mice used are free of pathogens, thereby the results obtained from this study do not account for the effects underlying infections may have on vaccine efficacy which is an important consideration for use in the human populations in developing countries that are most impacted by Schistosomiasis [177]. Using a different BCG reference strain could provide different immunological responses since large differences have been observed in the immunogenicity of BCG strains in BALB/c and C3H mice [178]. Future experiments should also

incorporate larger groups of mice and be repeated at least once. Since this study was a pilot experiment, the mice numbers were very small (ranging from 3 to 10 mice total per vaccine formulation type across both the immunogenicity and challenge experiments). Ten mice per group seems to be commonly used, however increasing the number of mice within each group can help statistically to reduce variance and increase confidence, making it easier to spot outliers and conduct a better analysis of the humoral, cell-mediated, and protective trends over time [179]. Furthermore, analyzing novel vaccine efficacy against challenge with related *Schistosoma* species may also prove informative. *S. mansoni*, *S. japonicum* and *S. haematobium* are responsible for most human infections, so analyzing BCG and cathepsin B specific to each species could demonstrate how broad the vaccines protection could be [180].

In conclusion, there are many additional reasons why research should be continued on the use of an *Sm*CB BCG vaccine candidate. Using BCG as a vaccine platform would be ideal for *Schistosoma* prone regions across global since most of them already have a universal BCG vaccination program in place [181]. Implementing BCG based vaccines is also more convenient than other vaccine platforms, such as RNA based vaccines, due to BCG's low cost, heat stability, easy mass production, along with its safety and reliability [93]. Although the BCG vaccine includes many benefits, including significantly reducing the risk of childhood TB, TB is still the leading infectious disease killer globally [182]. Although significant further research is required on the co-infection between TB and schistosomiasis, a recent systematic review observed that immunity against *S. mansoni* may increase latent TB reactivation through a Th1/Th2 switch, and that co-infection between these two diseases range anywhere between 4 to 34% [183]. Furthermore, a study in Kenya demonstrated that individuals infected with schistosomiasis have a higher chance of developing TB, especially if they were positive for HIV [184]. Schistosomiasis

comorbidities with infections such as TB and HIV are common in *Schistosoma* prone regions, lead to a much more severe disease outcome, and prove the importance of creating preventative vaccines for schistosomiasis and HIV, as well as ameliorating the BCG vaccine for TB. The promising advancement of recombinant BCG technology, along with the recent approval for the first ever parasitic vaccine, provides aspiration in creating a BCG *Sm*CB vaccine candidate that will hopefully bring an end to the suffering that hundreds of millions face from schistosomiasis and in turn other comorbid diseases such as TB and HIV.

Appendix

Supplemental Table 2.1: *Sm*CB sequence optimization for *M. tb.* Amino acids codons in the original obtained *Sm*CB DNA were analyzed and optimized to match the codon usage preference of *M. tb*. The original ratios of codons used are listed under original fraction (where each codon is a fraction, and all codons for one given amino acid add up to 1). The *M. tb* fraction lists the known ratio of each codon across the entire *M. tb* genome. The optimized fraction shows the codon ratios used in the final optimized *Sm*CB DNA.

Amino Acid		Codon	Number	Original Fraction	M. tb Fraction	Amino Acid	Codon	Number	Optimized Fraction
Ala	A	GCG	0	0	0.37	Ala	GCG	6	0.38
Ala	A	GCA	4	0.25	0.1	Ala	GCA	0	0
Ala	A	GCT	1	0.06	0.08	Ala	GCT	0	0
Ala	A	GCC	11	0.69	0.45	Ala	GCC	10	0.63
Cys	C	TGT	7	0.5	0.25	Cys	TGT	9	0.64
Cys	C	TGC	7	0.5	0.75	Cys	TGC	5	0.36
Asp	D	GAT	8	0.47	0.27	Asp	GAT	9	0.53
Asp	D	GAC	9	0.53	0.73	Asp	GAC	8	0.47
Glu	E	GAG	23	0.88	0.65	Glu	GAG	13	0.5
Glu	E	GAA	3	0.12	0.35	Glu	GAA	13	0.5
Phe	F	TTT	3	0.38	0.21	Phe	TTT	5	0.63
Phe	F	TTC	5	0.63	0.79	Phe	TTC	3	0.38
Gly	G	GGG	1	0.04	0.19	Gly	GGG	6	0.21
Gly	G	GGA	9	0.32	0.1	Gly	GGA	0	0
Gly	G	GGT	0	0	0.19	Gly	GGT	7	0.25
Gly	G	GGC	18	0.64	0.51	Gly	GGC	15	0.54
His	H	CAT	1	0.1	0.29	His	CAT	4	0.4
His	H	CAC	9	0.9	0.71	His	CAC	6	0.6
Ile	I	ATA	0	0	0.05	Ile	ATA	0	0
Ile	I	ATT	1	0.04	0.15	Ile	ATT	6	0.25
Ile	I	ATC	23	0.96	0.8	Ile	ATC	18	0.75
Lys	K	AAG	23	0.88	0.74	Lys	AAG	12	0.46
Lys	K	AAA	3	0.12	0.26	Lys	AAA	14	0.54
Leu	L	TTG	0	0	0.18	Leu	TTG	3	0.27

Leu	L	TTA	0	0	0.02	Leu	TTA	0	0
Leu	L	CTG	11	1	0.52	Leu	CTG	6	0.55
Leu	L	CTA	0	0	0.05	Leu	CTA	0	0
Leu	L	CTT	0	0	0.06	Leu	CTT	0	0
Leu	L	CTC	0	0	0.18	Leu	CTC	2	0.18
Met	M	ATG	3	1	1	Met	ATG	3	1
Asn	N	AAT	8	0.44	0.21	Asn	AAT	12	0.67
Asn	N	AAC	10	0.56	0.79	Asn	AAC	6	0.33
Pro	P	CCG	0	0	0.54	Pro	CCG	11	0.69
Pro	P	CCA	6	0.38	0.11	Pro	CCA	0	0
Pro	P	CCT	5	0.31	0.06	Pro	CCT	0	0
Pro	P	CCC	5	0.31	0.29	Pro	CCC	5	0.31
Gln	Q	CAG	8	1	0.74	Gln	CAG	5	0.63
Gln	Q	CAA	0	0	0.26	Gln	CAA	3	0.38
Arg	R	AGG	11	0.52	0.04	Arg	AGG	0	0
Arg	R	AGA	6	0.29	0.02	Arg	AGA	0	0
Arg	R	CGG	1	0.05	0.34	Arg	CGG	10	0.48
Arg	R	CGA	0	0	0.1	Arg	CGA	0	0
Arg	R	CGT	0	0	0.12	Arg	CGT	2	0.1
Arg	R	CGC	3	0.14	0.39	Arg	CGC	9	0.43
Ser	S	AGT	0	0	0.06	Ser	AGT	0	0
Ser	S	AGC	9	0.35	0.26	Ser	AGC	10	0.38
Ser	S	TCG	0	0	0.35	Ser	TCG	8	0.31
Ser	S	TCA	0	0	0.06	Ser	TCA	0	0
Ser	S	TCT	8	0.31	0.04	Ser	TCT	0	0
Ser	S	TCC	9	0.35	0.21	Ser	TCC	8	0.31
Thr	T	ACG	0	0	0.26	Thr	ACG	7	0.54
Thr	T	ACA	6	0.46	0.08	Thr	ACA	0	0
Thr	T	ACT	0	0	0.06	Thr	ACT	0	0
Thr	T	ACC	7	0.54	0.6	Thr	ACC	6	0.46
Val	V	GTG	13	0.93	0.47	Val	GTG	9	0.64

Val	V	GTA	0	0	0.06	Val	GTA	0	0
Val	V	GTT	0	0	0.09	Val	GTT	0	0
Val	V	GTC	1	0.07	0.38	Val	GTC	5	0.36

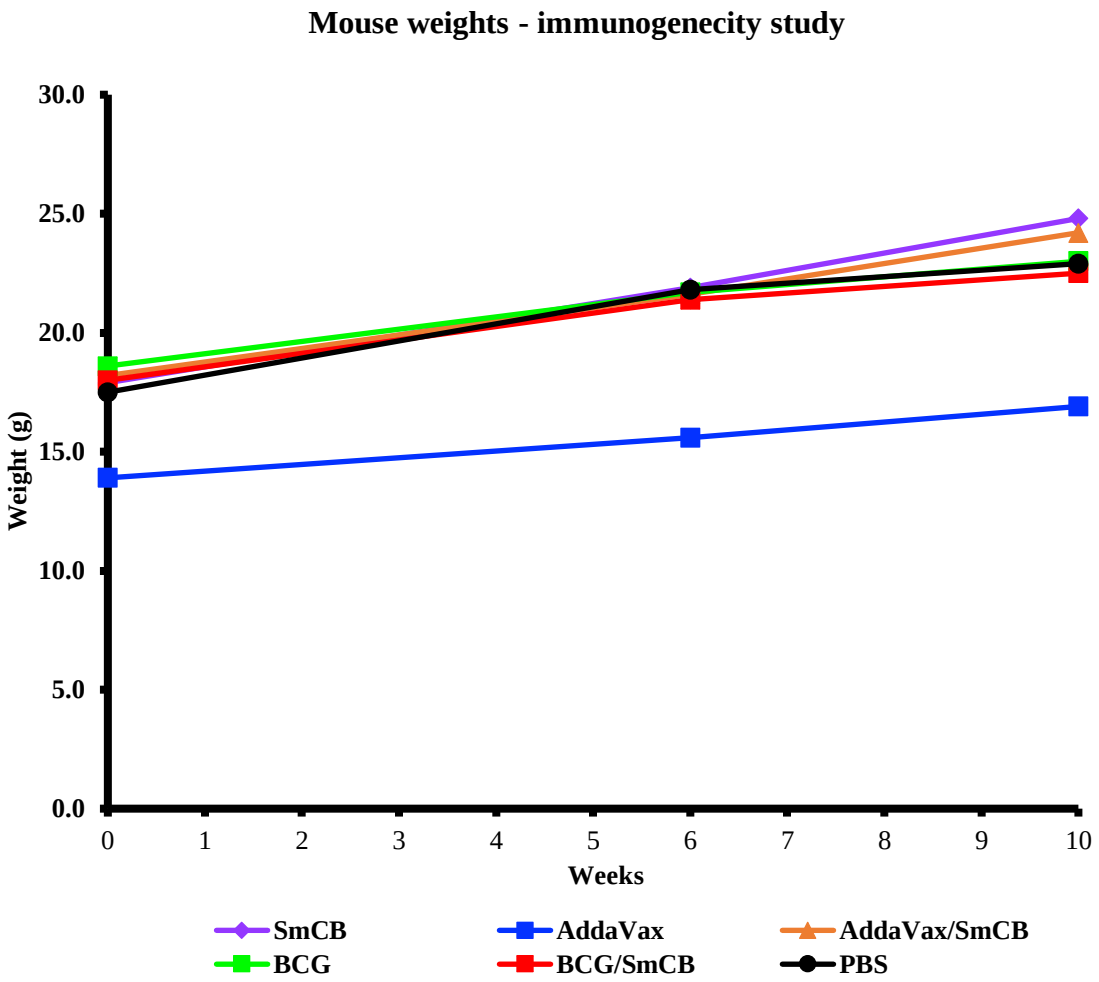

Supplemental Figure 3.1: Mouse weights for the immunogenicity study. Each line corresponds to the average weight of the mice within each vaccination group. Mice weights were taken at three time points: week 0, 6 and 10. Although the AddaVax mice group only contained 3 mice, which were on average approximately 3 grams lighter than the rest of the mice groups, their weights followed the same trend as the others.

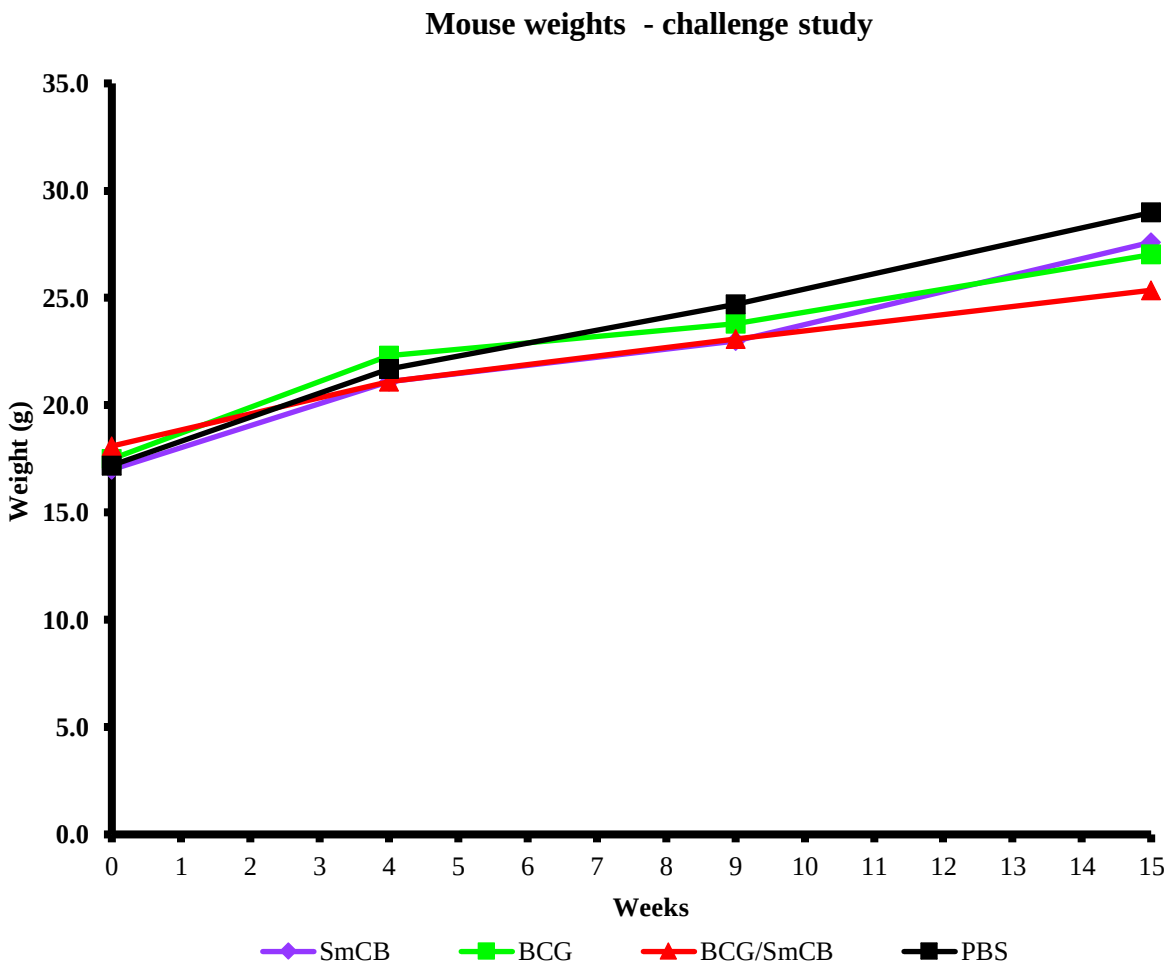

Supplemental Figure 3.1: Mouse weights challenge study. Each line corresponds to the average weight of the mice within each vaccination group. Mouse weights were taken at four time points: week 0, 4, 9 and 15.

References

1. Nelwan, M.L., *Schistosomiasis: Life Cycle, Diagnosis, and Control.* Curr Ther Res Clin Exp, 2019. **91**: p. 5-9.
2. Evan Secor, W., *Water-based interventions for schistosomiasis control.* Pathog Glob Health, 2014. **108**(5): p. 246-54.
3. *Current estimated total number of individuals with morbidity and mortality due to Schistosomiasis Haematobium and S. Mansoni infection in Sub-Saharan Africa.* World Health Organization, 2019.
4. Sánchez-Marqués, R., et al., *Research on Schistosomiasis in the Era of the COVID-19 Pandemic: A Bibliometric Analysis.* Int J Environ Res Public Health, 2022. **19**(13).
5. Kura, K., et al., *Disruptions to schistosomiasis programmes due to COVID-19: an analysis of potential impact and mitigation strategies.* Trans R Soc Trop Med Hyg, 2021. **115**(3): p. 236-244.
6. Olamiju, F., et al., *Schistosomiasis outbreak during COVID-19 pandemic in Takum, Northeast Nigeria: Analysis of infection status and associated risk factors.* PLoS One, 2022. **17**(1): p. e0262524.
7. Dejon-Agobé, J.C., et al., *Epidemiology of Schistosomiasis and Soil-Transmitted Helminth Coinfections among Schoolchildren Living in Lambaréné, Gabon.* Am J Trop Med Hyg, 2020. **103**(1): p. 325-333.
8. Colley, D.G., et al., *Human schistosomiasis.* Lancet, 2014. **383**(9936): p. 2253-64.
9. Sinuon, M., et al., *Control of Schistosoma mekongi in Cambodia: results of eight years of control activities in the two endemic provinces.* Transactions of the Royal Society of Tropical Medicine and Hygiene, 2007. **101**: p. 34-9.
10. Soares Magalhães, R.J., et al., *Geographical distribution of human Schistosoma japonicum infection in The Philippines: tools to support disease control and further elimination.* Int J Parasitol, 2014. **44**(13): p. 977-84.
11. Meurs, L., et al., *Micro-Geographical Heterogeneity in Schistosoma mansoni and S. haematobium Infection and Morbidity in a Co-Endemic Community in Northern Senegal.* PLOS Neglected Tropical Diseases, 2013. **7**(12): p. e2608.
12. Pinto-Almeida, A., et al., *Morphological Characteristics of Schistosoma mansoni PZQ-Resistant and -Susceptible Strains Are Different in Presence of Praziquantel.* Frontiers in microbiology, 2016. **7**: p. 594-594.
13. McManus, D.P., *Recent Progress in the Development of Liver Fluke and Blood Fluke Vaccines.* Vaccines, 2020. **8**(3): p. 553.
14. Nagi, S., et al., *Risk factors and spatial distribution of Schistosoma mansoni infection among primary school children in Mbita District, Western Kenya.* PLoS neglected tropical diseases, 2014. **8**(7): p. e2991-e2991.

15. Njunda, A.L., et al., *Prevalence and factors associated with urogenital schistosomiasis among primary school children in barrage, Magba sub-division of Cameroon.* BMC Public Health, 2017. **17**(1): p. 618.
16. Aula, O.P., et al., *Schistosomiasis with a Focus on Africa.* Trop Med Infect Dis, 2021. **6**(3).
17. Mortier, C., et al., *Schistosoma haematobium infection with pulmonary involvement in a traveller returning from Congo: A case report and systematic review of literature on nodular pulmonary schistosomiasis.* Travel Medicine and Infectious Disease, 2021. **44**: p. 102182.
18. El Ridi, R. and H. Tallima, *Why the radiation-attenuated cercarial immunization studies failed to guide the road for an effective schistosomiasis vaccine: A review.* J Adv Res, 2015. **6**(3): p. 255-67.
19. Ajibola, O., et al., *Tools for Detection of Schistosomiasis in Resource Limited Settings.* Medical sciences (Basel, Switzerland), 2018. **6**(2): p. 39.
20. Attallah, A.M., et al., *Fast-Dot ELISA using urine, a rapid and dependable field assay for diagnosis of schistosomiasis.* J Egypt Soc Parasitol, 1997. **27**(1): p. 279-89.
21. *Schistosomiasis - Parasite Biology - Life cycle.* Centers for Disease Control and Prevention, 2019.
22. Tucker, M.S., et al., *Schistosomiasis.* Curr Protoc Immunol, 2013. **103**: p. 19.1.1-19.1.58.
23. Loker, E.S., *A comparative study of the life-histories of mammalian schistosomes.* Parasitology, 1983. **87 (Pt 2)**: p. 343-69.
24. Furlong, S.T. and J.P. Caulfield, *Schistosoma mansoni: sterol and phospholipid composition of cercariae, schistosomula, and adults.* Exp Parasitol, 1988. **65**(2): p. 222-31.
25. Coakley, G., M.D. Wright, and J.G. Borger, *Schistosoma mansoni-Derived Lipids in Extracellular Vesicles: Potential Agonists for Eosinophillic Tissue Repair.* Front Immunol, 2019. **10**: p. 1010.
26. Zhu, B., et al., *Schistosoma japonicum cathepsin B2 (SjCB2) facilitates parasite invasion through the skin.* PLOS Neglected Tropical Diseases, 2020. **14**(10): p. e0008810.
27. Salter, J.P., et al., *Schistosome invasion of human skin and degradation of dermal elastin are mediated by a single serine protease.* J Biol Chem, 2000. **275**(49): p. 38667-73.
28. MacInnis, A.J., *Identification of chemicals triggering cercarial penetration responses of Schistosoma mansoni.* Nature, 1969. **224**(5225): p. 1221-2.
29. Hambrook, J.R. and P.C. Hanington, *Immune Evasion Strategies of Schistosomes.* Frontiers in Immunology, 2021. **11**.
30. Nation, C.S., et al., *Schistosome migration in the definitive host.* PLoS Negl Trop Dis, 2020. **14**(4): p. e0007951.
31. Wilson, R.A. and J.R. Lawson, *An examination of the skin phase of schistosome migration using a hamster cheek pouch preparation.* Parasitology, 1980. **80**(2): p. 257-66.
32. Gui, M., et al., *Schistosoma japonicum and S. mansoni: comparison of larval migration patterns in mice.* Journal of Helminthology, 1995. **69**(1): p. 19-25.

33. Lawson, J.R. and R.A. Wilson, *Metabolic changes associated with the migration of the schistosomulum of Schistosoma mansoni in the mammal host.* Parasitology, 1980. **81**(2): p. 325-36.
34. Wilson, R.A. and P.S. Coulson, *Immune effector mechanisms against schistosomiasis: looking for a chink in the parasite's armour.* Trends Parasitol, 2009. **25**(9): p. 423-31.
35. Dean, D.A. and B.L. Mangold, *Evidence that both normal and immune elimination of Schistosoma mansoni take place at the lung stage of migration prior to parasite death.* Am J Trop Med Hyg, 1992. **47**(2): p. 238-48.
36. Wheater, P.R. and R.A. Wilson, *Schistosoma mansoni: a histological study of migration in the laboratory mouse.* Parasitology, 1979. **79**(1): p. 49-62.
37. Abdelghani, E., et al., *Schistosomiasis and liver disease: Learning from the past to understand the present.* Clin Case Rep, 2020. **8**(8): p. 1522-1526.
38. Abath, F.G., et al., *Molecular approaches for the detection of Schistosoma mansoni: possible applications in the detection of snail infection, monitoring of transmission sites, and diagnosis of human infection.* Mem Inst Oswaldo Cruz, 2006. **101 Suppl 1**: p. 145-8.
39. Cheever, A.W., A.H. Torky, and M. Shirbiney, *The relation of worm burden to passage of Schistosoma haematobium eggs in the urine of infected patients.* Am J Trop Med Hyg, 1975. **24**(2): p. 284-8.
40. Pitchford, R.J., *DIFFERENCES IN THE EGG MORPHOLOGY AND CERTAIN BIOLOGICAL CHARACTERISTICS OF SOME AFRICAN AND MIDDLE EASTERN SCHISTOSOMES, GENUS SCHISTOSOMA, WITH TERMINAL-SPINED EGGS.* Bull World Health Organ, 1965. **32**(1): p. 105-20.
41. Wu, G.Y. and M.H. Halim, *Schistosomiasis: progress and problems.* World J Gastroenterol, 2000. **6**(1): p. 12-19.
42. Hassan, A.S., et al., *Therapeutic activity of a Salmonella-vectored Schistosoma mansoni vaccine in a mouse model of chronic infection.* Vaccine, 2021. **39**(39): p. 5580-5588.
43. Ross, A.G., et al., *Katayama syndrome.* Lancet Infect Dis, 2007. **7**(3): p. 218-24.
44. Logan, S., et al., *Acute schistosomiasis in travelers: 14 years' experience at the Hospital for Tropical Diseases, London.* Am J Trop Med Hyg, 2013. **88**(6): p. 1032-4.
45. McManus, D.P., et al., *Schistosomiasis in the People's Republic of China: the era of the Three Gorges Dam.* Clin Microbiol Rev, 2010. **23**(2): p. 442-66.
46. Macháček, T., et al., *Cercarial dermatitis: a systematic follow-up study of human cases with implications for diagnostics.* Parasitol Res, 2018. **117**(12): p. 3881-3895.
47. Ross, A.G., et al., *Schistosomiasis.* N Engl J Med, 2002. **346**(16): p. 1212-20.
48. Wamachi, A.N., et al., *Increased ratio of tumor necrosis factor-alpha to interleukin-10 production is associated with Schistosoma haematobium-induced urinary-tract morbidity.* J Infect Dis, 2004. **190**(11): p. 2020-30.
49. Neal, P.M., *Schistosomiasis--an unusual cause of ureteral obstruction: a case history and perspective.* Clin Med Res, 2004. **2**(4): p. 216-27.

50. Rollinson, D., et al., *Time to set the agenda for schistosomiasis elimination.* Acta Trop, 2013. **128**(2): p. 423-40.
51. Farah, I.O., et al., *Schistosoma mansoni: development and modulation of the granuloma after or multiple exposures in the baboon (Papio cynocephalus anubis).* Exp Parasitol, 1997. **86**(2): p. 93-101.
52. Martin, R.M., J.L. Brady, and A.M. Lew, *The need for IgG2c specific antiserum when isotyping antibodies from C57BL/6 and NOD mice.* J Immunol Methods, 1998. **212**(2): p. 187-92.
53. Santos, L.L., et al., *Urogenital Schistosomiasis-History, Pathogenesis, and Bladder Cancer.* J Clin Med, 2021. **10**(2).
54. Gobert, G.N., et al., *Adult schistosomes have an epithelial bacterial population distinct from the surrounding mammalian host blood.* PLoS One, 2022. **17**(1): p. e0263188.
55. Shebel, H.M., et al., *Genitourinary schistosomiasis: life cycle and radiologic-pathologic findings.* Radiographics, 2012. **32**(4): p. 1031-46.
56. Jourdan, P.M., et al., *HIV target cells in Schistosoma haematobium-infected female genital mucosa.* Am J Trop Med Hyg, 2011. **85**(6): p. 1060-4.
57. Bernardo, C., et al., *Insight into the molecular basis of Schistosoma haematobium-induced bladder cancer through urine proteomics.* Tumour Biol, 2016. **37**(8): p. 11279-87.
58. Kong, D.L., et al., *Soluble egg antigen of Schistosoma japonicum induces pyroptosis in hepatic stellate cells by modulating ROS production.* Parasit Vectors, 2019. **12**(1): p. 475.
59. Burke, M.L., et al., *Temporal Expression of Chemokines Dictates the Hepatic Inflammatory Infiltrate in a Murine Model of Schistosomiasis.* PLOS Neglected Tropical Diseases, 2010. **4**(2): p. e598.
60. Hams, E., G. Aviello, and P.G. Fallon, *The schistosoma granuloma: friend or foe?* Front Immunol, 2013. **4**: p. 89.
61. Phillips, S.M., et al., *Schistosomiasis in the congenitally athymic (nude) mouse. I. Thymic dependency of eosinophilia, granuloma formation, and host morbidity.* J Immunol, 1977. **118**(2): p. 594-9.
62. Dunne, D.W. and A. Cooke, *A worm's eye view of the immune system: consequences for evolution of human autoimmune disease.* Nat Rev Immunol, 2005. **5**(5): p. 420-6.
63. Rutitzky, L.I., H.J. Hernandez, and M.J. Stadecker, *Th1-polarizing immunization with egg antigens correlates with severe exacerbation of immunopathology and death in schistosome infection.* Proc Natl Acad Sci U S A, 2001. **98**(23): p. 13243-8.
64. Fallon, P.G., et al., *IL-4 Induces Characteristic Th2 Responses Even in the Combined Absence of IL-5, IL-9, and IL-13.* Immunity, 2002. **17**(1): p. 7-17.
65. Elias, D., et al., *Poor immunogenicity of BCG in helminth infected population is associated with increased in vitro TGF-beta production.* Vaccine, 2008. **26**(31): p. 3897-902.
66. Burke, M.L., et al., *Immunopathogenesis of human schistosomiasis.* Parasite Immunol, 2009. **31**(4): p. 163-76.

67. Dzhivhuho, G.A., et al., *Chronic schistosomiasis suppresses HIV-specific responses to DNA-MVA and MVA-gp140 Env vaccine regimens despite antihelminthic treatment and increases helminth-associated pathology in a mouse model.* PLOS Pathogens, 2018. **14**(7): p. e1007182.
68. Hinz, R., et al., *Serological approaches for the diagnosis of schistosomiasis – A review.* Molecular and Cellular Probes, 2017. **31**: p. 2-21.
69. Ricciardi, A., J.P. Dalton, and M. Ndao, *Evaluation of the immune response and protective efficacy of Schistosoma mansoni Cathepsin B in mice using CpG dinucleotides as adjuvant.* Vaccine, 2015. **33**(2): p. 346-53.
70. Gong, W., et al., *Protective immunity against Schistosoma japonicum infection can be provided by IgG antibodies towards periodate-sensitive or periodate-resistant glycans.* Parasites & Vectors, 2015. **8**(1): p. 234.
71. Coulson, P.S., *The radiation-attenuated vaccine against schistosomes in animal models: paradigm for a human vaccine?* Adv Parasitol, 1997. **39**: p. 271-336.
72. Park, S.K. and J.S. Marchant, *The Journey to Discovering a Flatworm Target of Praziquantel: A Long TRP.* Trends Parasitol, 2020. **36**(2): p. 182-194.
73. Cioli, D., et al., *Schistosomiasis control: praziquantel forever?* Mol Biochem Parasitol, 2014. **195**(1): p. 23-9.
74. Ricciardi, A., et al., *Immune Mechanisms Involved in Schistosoma mansoni-Cathepsin B Vaccine Induced Protection in Mice.* Front Immunol, 2018. **9**: p. 1710.
75. Wang, W., L. Wang, and Y.-S. Liang, *Susceptibility or resistance of praziquantel in human schistosomiasis: a review.* Parasitology Research, 2012. **111**(5): p. 1871-1877.
76. Johnston, E.A., J. Teague, and J.P. Graham, *Challenges and opportunities associated with neglected tropical disease and water, sanitation and hygiene intersectoral integration programs.* BMC Public Health, 2015. **15**(1): p. 547.
77. Bergquist, R. and D.J. Gray, *Schistosomiasis Elimination: Beginning of the End or a Continued March on a Trodden Path.* Trop Med Infect Dis, 2019. **4**(2).
78. Abd El-Aal, N.F., R.S. Hamza, and O. Harb, *Paeoniflorin targets apoptosis and ameliorates fibrosis in murine schistosomiasis mansoni: A novel insight.* Exp Parasitol, 2017. **183**: p. 23-32.
79. Molehin, A.J., *Current Understanding of Immunity Against Schistosomiasis: Impact on Vaccine and Drug Development.* Research and reports in tropical medicine, 2020. **11**: p. 119-128.
80. Zavala, F., *RTS,S: the first malaria vaccine.* J Clin Invest, 2022. **132**(1).
81. Datoo, M.S., et al., *Efficacy and immunogenicity of R21/Matrix-M vaccine against clinical malaria after 2 years' follow-up in children in Burkina Faso: a phase 1/2b randomised controlled trial.* The Lancet Infectious Diseases, 2022. **22**(12): p. 1728-1736.
82. Tebeje, B.M., et al., *Schistosomiasis vaccines: where do we stand?* Parasites & Vectors, 2016. **9**(1): p. 528.

83. Molehin, A.J., *Schistosomiasis vaccine development: update on human clinical trials.* Journal of Biomedical Science, 2020. **27**(1): p. 28.
84. Siddiqui, A.A., B.A. Siddiqui, and L. Ganley-Leal, *Schistosomiasis vaccines.* Hum Vaccin, 2011. **7**(11): p. 1192-7.
85. Jílková, A., M. Horn, and M. Mareš, *Structural and Functional Characterization of Schistosoma mansoni Cathepsin B1.* Methods Mol Biol, 2020. **2151**: p. 145-158.
86. Jílková, A., et al., *Activation route of the Schistosoma mansoni cathepsin B1 drug target: structural map with a glycosaminoglycan switch.* Structure, 2014. **22**(12): p. 1786-1798.
87. Nascimento, I.P. and L.C.C. Leite, *Recombinant vaccines and the development of new vaccine strategies.* Brazilian journal of medical and biological research = Revista brasileira de pesquisas medicas e biologicas, 2012. **45**(12): p. 1102-1111.
88. Ricciardi, A., et al., *A vaccine consisting of Schistosoma mansoni cathepsin B formulated in Montanide ISA 720 VG induces high level protection against murine schistosomiasis.* BMC Infect Dis, 2016. **16**: p. 112.
89. Hassan, A.S., et al., *Salmonella Typhimurium expressing chromosomally integrated Schistosoma mansoni Cathepsin B protects against schistosomiasis in mice.* npj Vaccines, 2023. **8**(1): p. 27.
90. Perera, D.J., et al., *Adjuvanted Schistosoma mansoni-Cathepsin B With Sulfated Lactosyl Archaeol Archaeosomes or AddaVax™ Provides Protection in a Pre-Clinical Schistosomiasis Model.* Frontiers in immunology, 2020. **11**: p. 605288-605288.
91. Calabro, S., et al., *The adjuvant effect of MF59 is due to the oil-in-water emulsion formulation, none of the individual components induce a comparable adjuvant effect.* Vaccine, 2013. **31**(33): p. 3363-9.
92. Fang, J.-H. and M. Hora, *The Adjuvant MF59: A 10-Year Perspective Gary Ott, Ramachandran Radhakrishnan,* in *Vaccine Adjuvants: Preparation Methods and Research Protocols*, D.T. O'Hagan, Editor. 2000, Springer New York: Totowa, NJ. p. 211-228.
93. Zimmermann, P., et al., *The influence of neonatal Bacille Calmette-Guérin (BCG) immunisation on heterologous vaccine responses in infants.* Vaccine, 2019. **37**(28): p. 3735-3744.
94. Kilpeläinen, A., et al., *Priming With Recombinant BCG Expressing Novel HIV-1 Conserved Mosaic Immunogens and Boosting With Recombinant ChAdOx1 Is Safe, Stable, and Elicits HIV-1-Specific T-Cell Responses in BALB/c Mice.* Frontiers in Immunology, 2019. **10**(923).
95. Trunk, G., M. Davidović, and J. Bohlius, *Non-Specific Effects of Bacillus Calmette-Guérin: A Systematic Review and Meta-Analysis of Randomized Controlled Trials.* Vaccines (Basel), 2023. **11**(1).
96. Uthayakumar, D., et al., *Non-specific Effects of Vaccines Illustrated Through the BCG Example: From Observations to Demonstrations.* Front Immunol, 2018. **9**: p. 2869.

97. Arts, R.J.W., et al., *BCG Vaccination Protects against Experimental Viral Infection in Humans through the Induction of Cytokines Associated with Trained Immunity.* Cell Host Microbe, 2018. **23**(1): p. 89-100.e5.
98. Kiravu, A., et al., *Bacille Calmette-Guerin Vaccine Strain Modulates the Ontogeny of Both Mycobacterial-Specific and Heterologous T Cell Immunity to Vaccination in Infants.* Front Immunol, 2019. **10**: p. 2307.
99. Borgers, K., et al., *Reference genome and comparative genome analysis for the WHO reference strain for Mycobacterium bovis BCG Danish, the present tuberculosis vaccine.* BMC genomics, 2019. **20**(1): p. 561-561.
100. Pearce, E.J., et al., *Induction of protective immunity against Schistosoma mansoni by vaccination with schistosome paramyosin (Sm97), a nonsurface parasite antigen.* Proceedings of the National Academy of Sciences, 1988. **85**(15): p. 5678.
101. Taylor, M.G., et al., *Production and testing of Schistosoma japonicum candidate vaccine antigens in the natural ovine host.* Vaccine, 1998. **16**(13): p. 1290-1298.
102. Dube, A., et al., *Vaccination of langur monkeys (Presbytis entellus) against Leishmania donovani with autoclaved L. major plus BCG.* Parasitology, 1998. **116 (Pt 3)**: p. 219-21.
103. Misra, A., et al., *Successful vaccination against Leishmania donovani infection in Indian langur using alum-precipitated autoclaved Leishmania major with BCG.* Vaccine, 2001. **19**(25-26): p. 3485-92.
104. Nahrevanian, H., et al., *Evaluation of anti-leishmanial effects of killed Leishmania vaccine with BCG adjuvant in BALB/c mice infected with Leishmania major MRHO/IR/75/ER.* Folia Parasitol (Praha), 2013. **60**(1): p. 1-6.
105. Joshi, S., et al., *Immunogenicity and Protective Efficacy of T-Cell Epitopes Derived From Potential Th1 Stimulatory Proteins of Leishmania (Leishmania) donovani.* Front Immunol, 2019. **10**: p. 288.
106. Mouhoub, E., et al., *The Diverse Applications of Recombinant BCG-Based Vaccines to Target Infectious Diseases Other Than Tuberculosis: An Overview.* Frontiers in Microbiology, 2021. **12**(3199).
107. Stover, C.K., et al., *New use of BCG for recombinant vaccines.* Nature, 1991. **351**(6326): p. 456-460.
108. Zheng, Y.Q., et al., *Applications of bacillus Calmette-Guerin and recombinant bacillus Calmette-Guerin in vaccine development and tumor immunotherapy.* Expert Rev Vaccines, 2015. **14**(9): p. 1255-75.
109. Varaldo, P.B., et al., *Recombinant Mycobacterium bovis BCG expressing the Sm14 antigen of Schistosoma mansoni protects mice from cercarial challenge.* Infect Immun, 2004. **72**(6): p. 3336-43.
110. Arama, C., et al., *A recombinant Bacille Calmette-Guérin construct expressing the Plasmodium falciparum circumsporozoite protein enhances dendritic cell activation and primes for circumsporozoite-specific memory cells in BALB/c mice.* Vaccine, 2012. **30**(37): p. 5578-84.

111. Ibrahim, H.M., et al., *Toxoplasma gondii cyclophilin 18-mediated production of nitric oxide induces Bradyzoite conversion in a CCR5-dependent manner.* Infect Immun, 2009. **77**(9): p. 3686-95.
112. Yu, Q., et al., *Protective immunity induced by a recombinant BCG vaccine encoding the cyclophilin gene of Toxoplasma gondii.* Vaccine, 2013. **31**(51): p. 6065-71.
113. Stover, C.K., et al., *New use of BCG for recombinant vaccines.* Nature, 1991. **351**(6326): p. 456-60.
114. Stover, C.K., et al., *Protective immunity elicited by recombinant bacille Calmette-Guerin (BCG) expressing outer surface protein A (OspA) lipoprotein: a candidate Lyme disease vaccine.* J Exp Med, 1993. **178**(1): p. 197-209.
115. Gomez, M., S. Johnson, and M.L. Gennaro, *Identification of secreted proteins of Mycobacterium tuberculosis by a bioinformatic approach.* Infect Immun, 2000. **68**(4): p. 2323-7.
116. Bendtsen, J.D., et al., *Non-classical protein secretion in bacteria.* BMC Microbiology, 2005. **5**(1): p. 58.
117. Feltcher, M.E., J.T. Sullivan, and M. Braunstein, *Protein export systems of Mycobacterium tuberculosis: novel targets for drug development?* Future microbiology, 2010. **5**(10): p. 1581-1597.
118. Zheng, Y.-q., et al., *Applications of bacillus Calmette-Guerin and recombinant bacillus Calmette-Guerin in vaccine development and tumor immunotherapy.* Expert review of vaccines, 2015. **14**(9): p. 1255-1275.
119. Movahedzadeh, F., R. Frita, and H.J. Gutka, *A two-step strategy for the complementation of M. tuberculosis mutants.* Genetics and molecular biology, 2011. **34**(2): p. 286-289.
120. Ohtsubo, K. and J.D. Marth, *Cre Recombinase Gene Transfer In Vitro and Detection of loxP-Dependent Recombination.* CSH Protoc, 2007. **2007**: p. pdb.prot4762.
121. Borsuk, S., et al., *Auxotrophic complementation as a selectable marker for stable expression of foreign antigens in Mycobacterium bovis BCG.* Tuberculosis (Edinb), 2007. **87**(6): p. 474-80.
122. Mignon, C., R. Sodoyer, and B. Werle, *Antibiotic-free selection in biotherapeutics: now and forever.* Pathogens (Basel, Switzerland), 2015. **4**(2): p. 157-181.
123. Zhou, Z.J., R. Qiu, and J. Zhang, *Molecular characterization of the cathepsin B of turbot (Scophthalmus maximus).* Fish Physiol Biochem, 2015. **41**(2): p. 473-83.
124. Livak, K.J. and T.D. Schmittgen, *Analysis of Relative Gene Expression Data Using Real-Time Quantitative PCR and the 2−ΔΔCT Method.* Methods, 2001. **25**(4): p. 402-408.
125. Hurst-Hess, K., et al., *Mycobacterial SigA and SigB Cotranscribe Essential Housekeeping Genes during Exponential Growth.* mBio, 2019. **10**(3).
126. Vinod, V., et al., *Interaction mechanism of Mycobacterium tuberculosis GroEL2 protein with macrophage Lectin-like, oxidized low-density lipoprotein receptor-1: An integrated computational and experimental study.* Biochim Biophys Acta Gen Subj, 2021. **1865**(1): p. 129758.

127. Sielaff, B., K.S. Lee, and F.T. Tsai, *Structural and functional conservation of Mycobacterium tuberculosis GroEL paralogs suggests that GroEL1 Is a chaperonin.* J Mol Biol, 2011. **405**(3): p. 831-9.
128. Hayer-Hartl, M., A. Bracher, and F.U. Hartl, *The GroEL-GroES Chaperonin Machine: A Nano-Cage for Protein Folding.* Trends in Biochemical Sciences, 2016. **41**(1): p. 62-76.
129. Reddy, P.T. and W.B. O'Dell, *Fusing an insoluble protein to GroEL apical domain enhances soluble expression in Escherichia coli.* Methods Enzymol, 2021. **659**: p. 171-188.
130. Sawyer, E.B., A.D. Grabowska, and T. Cortes, *Translational regulation in mycobacteria and its implications for pathogenicity.* Nucleic Acids Research, 2018. **46**(14): p. 6950-6961.
131. Soman, S., et al., *Codon optimality has minimal effect on determining translation efficiency in mycobacterium tuberculosis.* Scientific Reports, 2023. **13**(1): p. 415.
132. Korepanova, A., et al., *Expression of membrane proteins from Mycobacterium tuberculosis in Escherichia coli as fusions with maltose binding protein.* Protein Expr Purif, 2007. **53**(1): p. 24-30.
133. Brondyk, W.H., *Chapter 11 Selecting an Appropriate Method for Expressing a Recombinant Protein*, in *Methods in Enzymology*, R.R. Burgess and M.P. Deutscher, Editors. 2009, Academic Press. p. 131-147.
134. Wiśniewski, J.R. and M. Mann, *A Proteomics Approach to the Protein Normalization Problem: Selection of Unvarying Proteins for MS-Based Proteomics and Western Blotting.* Journal of Proteome Research, 2016. **15**(7): p. 2321-2326.
135. Watanabe, H., et al., *Innate immune response in Th1- and Th2-dominant mouse strains.* Shock, 2004. **22**(5): p. 460-6.
136. Johnson, M., *Laboratory Mice and Rats.* Materials and Methods, 2012.
137. Perera, D.J., et al., *Adjuvanted Schistosoma mansoni-Cathepsin B With Sulfated Lactosyl Archaeol Archaeosomes or AddaVax™ Provides Protection in a Pre-Clinical Schistosomiasis Model.* Frontiers in Immunology, 2020. **11**.
138. Lewis, F., *Schistosomiasis.* Curr Protoc Immunol, 2001. **Chapter 19**: p. Unit 19.1.
139. Schulze, T.T., et al., *Mouse splenocyte enrichment strategies via negative selection for broadened single-cell transcriptomics.* STAR Protocols, 2022. **3**(2): p. 101402.
140. Yam, K.K., et al., *AS03-Adjuvanted, Very-Low-Dose Influenza Vaccines Induce Distinctive Immune Responses Compared to Unadjuvanted High-Dose Vaccines in BALB/c Mice.* Frontiers in Immunology, 2015. **6**.
141. Agallou, M. and E. Karagouni, *Detection of Antigen-specific T cells in Spleens of Vaccinated Mice Applying (3)[H]-Thymidine Incorporation Assay and Luminex Multiple Cytokine Analysis Technology.* Bio Protoc, 2019. **9**(11): p. e3252.
142. Kremer, L., et al., *Neutralizing antibody responses elicited in mice immunized with recombinant bacillus Calmette-Guérin producing the Schistosoma mansoni glutathione S-transferase.* J Immunol, 1996. **156**(11): p. 4309-17.

143. Stils, H.F., Jr., *Adjuvants and Antibody Production: Dispelling the Myths Associated with Freund's Complete and Other Adjuvants.* ILAR Journal, 2005. **46**(3): p. 280-293.
144. Saroha, M., et al., *Immunogenicity and safety of early vs delayed BCG vaccination in moderately preterm (31-33 weeks) infants.* Hum Vaccin Immunother, 2015. **11**(12): p. 2864-71.
145. Dalmia, N. and A.J. Ramsay, *Prime-boost approaches to tuberculosis vaccine development.* Expert Rev Vaccines, 2012. **11**(10): p. 1221-33.
146. Brady, S.M., et al., *Reassess the t Test: Interact with All Your Data via ANOVA.* The Plant Cell, 2015. **27**(8): p. 2088-2094.
147. Nazeri, S., et al., *Measuring of IgG2c isotype instead of IgG2a in immunized C57BL/6 mice with Plasmodium vivax TRAP as a subunit vaccine candidate in order to correct interpretation of Th1 versus Th2 immune response.* Exp Parasitol, 2020. **216**: p. 107944.
148. Witschkowski, J., et al., *BCG Provides Short-Term Protection from Experimental Cerebral Malaria in Mice.* Vaccines (Basel), 2020. **8**(4).
149. Raphael, I., et al., *T cell subsets and their signature cytokines in autoimmune and inflammatory diseases.* Cytokine, 2015. **74**(1): p. 5-17.
150. Sakamoto, S., et al., *Enzyme-linked immunosorbent assay for the quantitative/qualitative analysis of plant secondary metabolites.* J Nat Med, 2018. **72**(1): p. 32-42.
151. Arango Duque, G. and A. Descoteaux, *Macrophage cytokines: involvement in immunity and infectious diseases.* Front Immunol, 2014. **5**: p. 491.
152. Zhou, F., *Molecular mechanisms of IFN-gamma to up-regulate MHC class I antigen processing and presentation.* Int Rev Immunol, 2009. **28**(3-4): p. 239-60.
153. Marchant, A., et al., *Newborns develop a Th1-type immune response to Mycobacterium bovis bacillus Calmette-Guérin vaccination.* J Immunol, 1999. **163**(4): p. 2249-55.
154. Jiang, X., et al., *Non-Specific Binding and Cross-Reaction of ELISA: A Case Study of Porcine Hemoglobin Detection.* Foods, 2021. **10**(8).
155. Pearce, E.J., et al., *Th2 response polarization during infection with the helminth parasite Schistosoma mansoni.* Immunol Rev, 2004. **201**: p. 117-26.
156. Nian, X., et al., *AddaVax Formulated with PolyI:C as a Potential Adjuvant of MDCK-based Influenza Vaccine Enhances Local, Cellular, and Antibody Protective Immune Response in Mice.* AAPS PharmSciTech, 2021. **22**(8): p. 270.
157. Calabro, S., et al., *The adjuvant effect of MF59 is due to the oil-in-water emulsion formulation, none of the individual components induce a comparable adjuvant effect.* Vaccine, 2013. **31**(33): p. 3363-3369.
158. Chen, Y.-J., et al., *Development of a highly sensitive enzyme-linked immunosorbent assay (ELISA) through use of poly-protein G-expressing cell-based microplates.* Scientific Reports, 2018. **8**(1): p. 17868.
159. Wang, J., et al., *Monitoring specific antibody responses against the hydrophilic domain of the 23 kDa membrane protein of Schistosoma japonicum for early detection of infection in sentinel mice.* Parasites & Vectors, 2011. **4**(1): p. 172.

160. Kiflie, A., et al., *Helminth species-specific effects on IFN-γ producing T cells during active and latent tuberculosis.* PLOS Neglected Tropical Diseases, 2023. **17**(1): p. e0011094.
161. Schramm, G., et al., *Cutting edge: IPSE/alpha-1, a glycoprotein from Schistosoma mansoni eggs, induces IgE-dependent, antigen-independent IL-4 production by murine basophils in vivo.* J Immunol, 2007. **178**(10): p. 6023-7.
162. Poole, J.A. and L.J. Rosenwasser, *The role of immunoglobulin E and immune inflammation: implications in allergic rhinitis.* Curr Allergy Asthma Rep, 2005. **5**(3): p. 252-8.
163. Gryseels, B., *Human resistance to Schistosoma infections: age or experience?* Parasitol Today, 1994. **10**(10): p. 380-4.
164. Dunne, D.W., et al., *Immunity after treatment of human schistosomiasis: association between IgE antibodies to adult worm antigens and resistance to reinfection.* Eur J Immunol, 1992. **22**(6): p. 1483-94.
165. Pinot de Moira, A., et al., *Analysis of complex patterns of human exposure and immunity to Schistosomiasis mansoni: the influence of age, sex, ethnicity and IgE.* PLoS Negl Trop Dis, 2010. **4**(9).
166. Diemert, D.J., et al., *Generalized urticaria induced by the Na-ASP-2 hookworm vaccine: implications for the development of vaccines against helminths.* J Allergy Clin Immunol, 2012. **130**(1): p. 169-76.e6.
167. Maizels, R.M. and H.J. McSorley, *Regulation of the host immune system by helminth parasites.* J Allergy Clin Immunol, 2016. **138**(3): p. 666-675.
168. Larkin, B.M., et al., *Induction and regulation of pathogenic Th17 cell responses in schistosomiasis.* Semin Immunopathol, 2012. **34**(6): p. 873-88.
169. Shainheit, M.G., et al., *Dendritic cell IL-23 and IL-1 production in response to schistosome eggs induces Th17 cells in a mouse strain prone to severe immunopathology.* J Immunol, 2008. **181**(12): p. 8559-67.
170. Bourke, C.D., et al., *Integrated Analysis of Innate, Th1, Th2, Th17, and Regulatory Cytokines Identifies Changes in Immune Polarisation Following Treatment of Human Schistosomiasis.* The Journal of Infectious Diseases, 2012. **208**(1): p. 159-169.
171. Allen, J.E. and R.M. Maizels, *Diversity and dialogue in immunity to helminths.* Nat Rev Immunol, 2011. **11**(6): p. 375-88.
172. Daly, D.S., et al., *Evaluating concentration estimation errors in ELISA microarray experiments.* BMC Bioinformatics, 2005. **6**: p. 17.
173. Herati, R.S. and E.J. Wherry, *What Is the Predictive Value of Animal Models for Vaccine Efficacy in Humans? Consideration of Strategies to Improve the Value of Animal Models.* Cold Spring Harb Perspect Biol, 2018. **10**(4).
174. Kowalewicz-Kulbat, M. and C. Locht, *Recombinant BCG to Enhance Its Immunomodulatory Activities.* Vaccines, 2022. **10**(5): p. 827.

175. Perera, D.J., et al., *A low dose adenovirus vectored vaccine expressing Schistosoma mansoni Cathepsin B protects from intestinal schistosomiasis in mice.* EBioMedicine, 2022. **80**: p. 104036.
176. Kruisbeek, A.M., *Commonly used mouse strains.* Curr Protoc Immunol, 2001. **Appendix 1**: p. Appendix 1C.
177. Ricciardi, A. and M. Ndao, *Still hope for schistosomiasis vaccine.* Hum Vaccin Immunother, 2015. **11**(10): p. 2504-8.
178. Lagranderie, M.R., et al., *Comparison of immune responses of mice immunized with five different Mycobacterium bovis BCG vaccine strains.* Infect Immun, 1996. **64**(1): p. 1-9.
179. Charan, J. and N.D. Kantharia, *How to calculate sample size in animal studies?* J Pharmacol Pharmacother, 2013. **4**(4): p. 303-6.
180. *Schistosomiasis and soil-transmitted helminthiases: number of people treated in 2015.* Wkly Epidemiol Rec, 2016. **91**(49-50): p. 585-95.
181. Zwerling, A., et al., *The BCG World Atlas: a database of global BCG vaccination policies and practices.* PLoS Med, 2011. **8**(3): p. e1001012.
182. Zhang, T., et al., *The global, regional, and national burden of tuberculosis in 204 countries and territories, 1990-2019.* J Infect Public Health, 2023. **16**(3): p. 368-375.
183. Baya, B., et al., *Prevalence and Clinical Relevance of Schistosoma mansoni Co-Infection with Mycobacterium tuberculosis: A Systematic Literature Review.* Open J Epidemiol, 2023. **13**(1): p. 97-111.
184. McLaughlin, T.A., et al., *Schistosoma mansoni Infection Is Associated With a Higher Probability of Tuberculosis Disease in HIV-Infected Adults in Kenya.* J Acquir Immune Defic Syndr, 2021. **86**(2): p. 157-163.